Cyclopentadienyl and Olefin Substituent Effects on Insertion and β-Hydrogen Elimination with Group 4 Metallocenes. Kinetics, Mechanism, and Thermodynamics for Zirconocene and Hafnocene Alkyl Hydride Derivatives

Paul J. Chirik† and John E. Bercaw*

Arnold and Mabel Beckman Laboratories of Chemical Synthesis, California Institute of Technology, Pasadena, California 91125

Received June 21, 2005

Reactions of group 4 metallocene dihydrides, $(R_nCp)_2MH_2$ (R_nCp = alkyl-substituted cyclopentadienyl; M = Zr, Hf), with olefins afford stable metallocene alkyl hydride complexes of the general formula $(R_nCp)_2M(CH_2CHR'_2)(H)$ (R′ = H, alkyl). For sterically crowded, monomeric dihydrides, $Cp^*_2ZrH_2$ ($Cp^* = \eta^5$-C_5Me_5), $Cp^*(\eta^5$-$C_5Me_4H)ZrH_2$, $Cp^*(\eta^5$-$C_5Me_4Et)$-ZrH_2, $Cp^*_2HfH_2$, and $Cp^*(\eta^5$-C_5H_3-1,3-$(CMe_3)_2)HfH_2$, second-order rate constants for olefin insertion have been measured. For $Cp^*_2HfH_2$, the relative rates of olefin insertion have been found to be 1-pentene > styrene ≫ *cis*-2-butene > cyclopentene > *trans*-2-butene > isobutene. The rate of isobutene insertion into $Cp^*(\eta^5$-$C_5Me_4H)ZrH_2$ is 3.8×10^3 times greater than that for $Cp^*_2ZrH_2$ at −63 °C, demonstrating the striking steric effect for isobutene insertion imposed by a tenth methyl substituent on the two cyclopentadienyl ligands. A primary k_H/k_D of 2.4(3) at 23 °C and a linear free energy correlation to σ ($\rho = -0.46(1)$) for *para*-substituted styrene insertion indicate that insertion into a Zr−H bond proceeds via rate-determining hydride transfer to coordinated olefin, with small positive charge buildup at the β-carbon of the inserting styrene. The rates of β-H elimination for the series $(R_n$-$Cp)_2Zr(CH_2CHR')(H)$ have been measured via rapid trapping of the intermediate zirconocene dihydride with 4,4-dimethyl-2-pentyne. Key observations for β-H elimination are (a) primary kinetic deuterium isotope effects ($k_H/k_D = 3.9-4.5$) and (b) a linear free relationship for the phenethyl hydride series $Cp^*(\eta^5$-$C_5Me_4H)Zr(CH_2CH_2$-p-C_6H_4-X)(H) (X = H, CH_3, CF_3, OCH_3), which correlates better to σ than σ^+; $\rho = -1.80(5)$. The rate of β-H elimination slows with more substituted, hence more sterically crowded, cyclopentadienyl ligands. Equilibration of a series of $Cp^*(CpR_n)Zr(CH_2CHMe_2)(H)$ and $Cp^*(CpR_n)Zr(CH_2CH_2CH_2CH_3)(H)$ with free isobutene and 1-butene has established the relative ground-state energies of isobutyl and *n*-butyl complexes. These data, in combination with the free energies of activation for β-H elimination, allow free energy profiles to be constructed for insertion and β-H elimination for each olefin.

Introduction

Olefin insertion into a metal−hydrogen bond and its microscopic reverse, β-H elimination from a transition metal alkyl, represent fundamental transformations in organometallic chemistry and constitute key steps in a variety of catalytic processes.[1] Olefin insertion and β-H elimination have special relevance to metallocene-catalyzed olefin polymerization; β-H elimination is a major chain transfer pathway, and insertion of an olefin into a metal−hydrogen bond is an important (re)-initiation step.[2] Under typical polymerization conditions the relative rates of chain propagation and β-H elimination determine polymer chain length and hence influence many important polyolefin properties.

Although the effect of metallocene symmetry on polymer stereochemistry is fairly well-understood,[3] a predictive correlation between cyclopentadienyl substitution pattern and polymer molecular weight has not yet been established. Commercial application of current metallocene catalysts is often hampered by the low polymer molecular weights, especially when the polymerization reaction is carried out at plant operating temperatures (normally greater than 60−80 °C for polypropylene).[4] End group analysis of these polymers reveals that chain termination occurs primarily by β-H and β-methyl elimination pathways. Hence, mechanistic understanding of each of the fundamental transformations comprising olefin polymerization, and correlation

* To whom correspondence should be addressed. E-mail: bercaw@caltech.edu.

† Current address: Department of Chemistry and Chemical Biology, Cornell University, Ithaca, NY 14853-1301.

(1) Crabtree, R. H. *The Organometallic Chemistry of the Transition Metals*, 2nd ed.; Wiley: New York, 1994; Chapters 7, 9.

(2) Brintzinger, H. H.; Fischer, D.; Mülhaupt, R.; Rieger, B.; Waymouth, R. M. *Angew. Chem., Int. Ed. Engl.* **1995**, *34*, 1143.

(3) (a) Gilchrist, J. H.; Bercaw, J. E. *J. Am. Chem. Soc.* **1996**, *118*, 12021. (b) Herzog, T. A.; Zubris, D. L.; Bercaw, J. E. *J. Am. Chem. Soc.* **1996**, *118*, 11988, and references therein.

(4) Resconi, L.; Camurati, I.; Sudmeijer, O. *Top. Catal.* **1999**, *7*, 145.

10.1021/om0580351 CCC: $30.25
Publication on Web 09/23/2005

of their rates as the cyclopentadienyl ligand substituents are varied (albeit a daunting prospect!), may lead to the development of metallocene catalysts that can be tailored to produce polymers with desired stereochemistry and molecular weight.

Olefin insertion and β-H elimination reactions for metallocenes have been the subject of several experimental and theoretical investigations.[5−7] Previous investigations from our research group have focused on understanding the kinetics and mechanism of olefin insertion and β-H elimination for metallocene catalysts. Using both coalesence and magnetization transfer NMR techniques, the kinetics of olefin insertion into a metal−hydrogen bond has been examined with a series of group 5 metallocene complexes of the general formula (η^5-$C_5R_5)_2M(\eta^2$-$CH_2{=}CHR')(H)$ (M = Nb, Ta; R = H, Me; R′ = H, CH_3, C_6H_5).[8] For the series of ethylene hydride compounds, increased rates of insertion were observed for niobium relative to tantalum and for less congested cyclopentadienyl relative to Cp* ligands (Cp* = η^5-C_5Me_5). Similar effects are also observed in the propylene hydride and styrene hydride complexes, although the steric effects dominate the electronic contributions. Permethylscandocene complexes, Cp^*_2ScR (R = H, alkyl), insert ethylene rapidly at low temperature (−80 °C) and without complication from chain transfer by β-H elimination. Hence, the kinetics of ethylene insertion has been measured for a series of scandium alkyls. The rates of ethylene insertion are affected by the strength of the scandium−carbon bond, where generally stronger bonds result in slower rates.[9] The rates of β-H elimination for a variety of scandium alkyls and phenethyl complexes have been determined via rapid trapping of the scandium hydride with 2-butyne. The relative free energies of the transition states for β-H elimination, and hence that for olefin insertion, have been probed by systematically varying the substituent at the β-carbon. As with the niobocene styrene hydride complexes, a linear free energy correlation was found for this scandium-phenethyl series, indicating a quite polar transition state with (in the limiting picture) the electropositive scandium center abstracting hydride of the positively charged β-carbon atom.

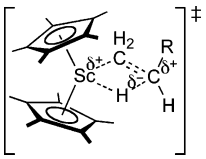

More recent studies have focused on elucidating the rates of chain propagation and transfer in cationic zirconocene catalysts. Erker has reported an experimental estimate for olefin insertion into cationic zirconium allyl fragments,[10] whereas Siedle has determined the relative rates of chain propagation and transfer for zirconocenedimethyl/methylalumoxane mixtures.[11] There were few direct *kinetic* studies employing relevant models for the propagating species,[12,13] until reports by Landis and co-workers, using quenched-flow kinetics and direct NMR methods, have measured elementary rate laws and rate constants for an *ansa*-zirconocene catalyst [*rac*-C_2H_4(1-indenyl)$_2$Zr(CH_3)][$CH_3B(C_6F_5)_3$],[14] and by Casey, using direct NMR methods to establish the relative rates for α-olefin insertion for Cp^*_2Y-CH_2-$(CH_2)_nCHMe_2$ (n = 0, 1).[15] Our group has very recently completed an investigation of chain initiation and propagation kinetics for [Cp*CpZr(CH_2CMe_3)][CH_3B-$(C_6F_5)_3$].[16]

These measurements have provided important information concerning the rate laws and rates for initiation, propagation, and chain transfer for these catalyst systems. Additionally, numerous theoretical studies have been aimed toward understanding the rates and mechanisms of these fundamental transformations.[17] Although the effect of cyclopentadienyl substitution on the stereo- and regiochemical outcome of a metallocene-catalyzed polymerization has been well documented,[18] less clear is how the catalyst structure influences the rates of olefin insertion and β-H elimination. Using 16-electron zirconocene and hafnocene dihydride and alkyl hydride complexes as models for the active polymerization catalyst (currently presumed to be a 16-electron, cationic polymeryl-solvento adduct or -contact ion pair), we have measured the rates and investigated mechanisms of olefin insertion and β-H elimination in order to assess the effects of ancillary cyclopentadienyl ligand substitution on the rates of these processes. As part of these investigations we found it possible to cleanly equilibrate a series of Cp*(CpR_n)Zr(CH_2CHMe_2)(H) and Cp*(CpR_n)Zr($CH_2CH_2CH_2CH_3$)(H) complexes with free isobutene and 1-butene, allowing thermodynamic and kinetic data to be extracted. These establish relative ground-state energies and thus, in combination with the free energies of activation for β-H elimination, permit free energy profiles to be constructed for insertion and β-H elimination for 1-butene versus isobutene.

(5) (a) Jordan, R. F.; Dasher, W. E.; Echols, S. F. *J. Am. Chem. Soc.* **1986**, *108*, 1718. (b) Jordan, R. F.; Bajgur, C. S.; Willet, R.; Scott, B. *J. Am. Chem. Soc.* **1986**, *108*, 7410.

(6) Watson, P. L. *J. Am. Chem. Soc.* **1982**, *104*, 337.

(7) Jeske, G.; Lauke, H.; Mauerman, H.; Swepston, P. N.; Shuman, H.; Marks, T. J. *J. Am. Chem. Soc.* **1985**, *107*, 8091.

(8) (a) Doherty, N. M.; Bercaw, J. E. *J. Am. Chem. Soc.* **1985**, *107*, 2670. (b) Burger, B. J.; Santarsiero, B. D.; Trimmer, M. S.; Bercaw, J. E. *J. Am. Chem. Soc.* **1988**, *110*, 3134.

(9) Burger, B. J.; Thompson, M. E.; Cotter, W. D.; Bercaw, J. E. *J. Am. Chem. Soc.* **1990**, *112*, 1566.

(10) Karl, J.; Dahlmann, M.; Erker, G.; Bergander, K. *J. Am. Chem. Soc.* **1998**, *120*, 5643.

(11) Siedle, A. R.; Lamanna, W. M.; Newmark, R. A.; Schroepfer, J. N. *J. Mol. Catal. A* **1998**, *128*, 257.

(12) Beswick, C. L.; Marks, T. J. *J. Am. Chem. Soc.* **2000**, *122*, 10358.

(13) (a) Casey, C. P.; Carpenetti, D. W., II; Sakurai, H. *J. Am. Chem. Soc.* **1999**, *121*, 9483−9484. (b) Casey, C. P.; Carpenetti, D. W., II. *Organometallics* **2000**, *19*, 3970−3977. (c) Brandow, C. G.; Mendiratta, A.; Bercaw, J. E. *Organometallics* **2001**, *20*, 4253. (d) Casey, C. P.; Carpenetti, D. W.; Sakurai, H. *Organometallics* **2001**, *20*, 4262−4265.

(14) (a) Sillars, D. R.; Landis, C. R. *J. Am. Chem. Soc.* **2003**, *125*, 9894. (b) Landis, C. R.; Rosaaen, K. A.; Sillars, D. R. *J. Am. Chem. Soc.* **2003**, *125*, 1710.

(15) Casey, C. P.; Tunge, J. A.; Lee, T. Y.; Fagan, M. A. *J. Am. Chem. Soc.* **2003**, *125*, 2641−2651.

(16) Klamo, S. K.; Bercaw, J. E. *J. Am. Chem. Soc.*, submitted for publication.

(17) (a) Woo, T. K.; Margl, P. M.; Lohrenz, J. C. W.; Blöchl, P. E.; Ziegler, T. *J. Am. Chem. Soc.* **1996**, *118*, 13021. (b) Richardson, D. E.; Alameddin, N. G.; Ryan, M. F.; Hayes, T.; Eyler, J. R.; Siedle, A. R. *J. Am. Chem. Soc.* **1996**, *118*, 11244. (c) Froese, R. D. J.; Musaev, D. G.; Matsubara, T.; Morokuma, K. J. *Organometallics* **1997**, *16*, 2514, and references therein.

(18) (a) Toto, M.; Cavallo, L.; Corradini, P.; Moscardi, G.; Resconi, L.; Guerra, G. *Macromolecules* **1998**, *31*, 3431. (b) Röll, W.; Brintzinger, H. H.; Rieger, B.; Zolk, R. *Angew. Chem., Int. Ed. Engl.* **1990**, *29*, 279. (c) Gilchrist, J. H.; Bercaw, J. E. *J. Am. Chem. Soc.* **1996**, *118*, 12021. (d) Coates G. W. *Chem. Rev.* **2000**, *100*, 1223. (e) Resconi, L.; Cavallo, L.; Fait, A.; Piemontesi, F. *Chem. Rev.* **2000**, *100*, 1253.

Table 1. Rate Constants for Insertion of Disubstituted Olefins CH_2=$C(CH_3)R$ with $Cp^*_2ZrH_2$ (1) at 23 °C

olefin substituent R	product	$k_{ins} \times 10^4$ (M^{-1} s^{-1})
CH_3	$Cp^*_2Zr(CH_2CHMe_2)(H)$ (**3**)	65(3)
CH_2CH_3	$Cp^*_2Zr\{CH_2CH(CH_3)(CH_2CH_3)\}(H)$ (**4**)	24(3)
$CH(CH_3)CH_2CH_3$	$Cp^*_2Zr\{CH_2CH(CH_3)CH(CH_3)CH_2CH_3\}(H)$ (**6**)	7.3(2)
CH_2CHMe_2	$Cp^*_2Zr\{CH_2CH(CH_3)CH_2CHMe_2\}(H)$ (**5**)	6.3(4)
C_6H_5	$Cp^*_2Zr\{CH_2CH(CH_3)(C_6H_5)\}(H)$ (**7**)	14(2)
CH_2CMe_3		no insertion

Results

Reactions of the metallocene dihydride complexes $(CpR_n)_2MH_2$[19] (CpR_n = alkyl-substituted cyclopentadienyl; M = Zr, Hf) with olefins such as propylene, 1-butene, and isobutene afford stable metallocene alkyl hydride complexes, $(CpR_n)_2M(CH_2CHR'_2)(H)$ (R′ = alkyl), in quantitative yield (by NMR) (eq 1). In general, the remaining metal−hydride bond is unreactive toward excess olefin.[20] The metallocene alkyl hydride complexes are stable in benzene-d_6 for days at 25 °C.

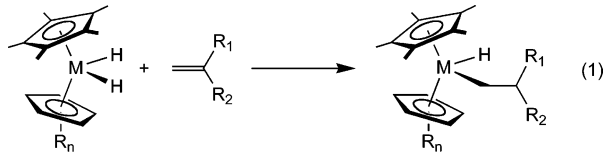

Kinetics of the Reactions of Olefins with $Cp^*_2MH_2$ Complexes. Permethylzirconocene dihydride, $Cp^*_2ZrH_2$ (**1**), and permethylhafnocene dihydride, $Cp^*_2HfH_2$ (**2**), are monomeric in benzene-d_6 solution, and thus the kinetics of their insertion reactions with olefins are straightforward to interpret. Reactions of **1** and **2** with 1,1-disubstituted olefins (e.g., isobutene) and α-olefins are first order in both olefin and the metallocene dihydride (eq 2). To probe olefin steric effects on the rate of insertion, reaction of **1** with a variety of 1,1-disubstituted olefins has been examined. Thus reaction of **1** with isobutene, 2-methyl-1-butene, 2,4-dimethyl-1-pentene, 2,3-dimethyl-1-pentene, and α−methylstyrene yields $Cp^*_2Zr(CH_2CHMe_2)(H)$ (**3**), $Cp^*_2Zr\{CH_2CH(CH_3)(CH_2CH_3)\}(H)$ (**4**), $Cp^*_2Zr\{CH_2CH(CH_3)CH_2CHMe_2\}(H)$ (**5**), $Cp^*_2Zr\{CH_2CH(CH_3)CH(CH_3)CH_2CH_3\}(H)$ (**6**), and $Cp^*_2Zr(CH_2CH(CH_3)(C_6H_5))(H)$ (**7**), respectively. The rate constants for these reactions have been measured at 23 °C, and the second-order rate constants (k_{ins}) are presented in Table 1. Reaction of **1** with 2,4,4-trimethyl-1-pentene produces no reaction. Likewise no alkane is observed upon attempted hydrogenation of this olefin with **1** as the catalyst.

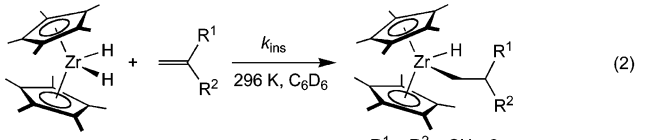

The effect of solvent on the rate of isobutene insertion with **1** has also been examined. The experimentally determined rate constants for the insertion reaction have been measured in a number of deuterated solvents at 23 °C, and these values are contained in Table 2. The extreme reactivity of the Zr−H bonds of **1** toward most functional groups limits the range of solvents that could be examined, however.

Table 2. Rate Constants as a Function of Solvent for Reaction of $Cp^*_2ZrH_2$ (1) with Isobutene at 23 °C

solvent	$k_{ins} \times 10^4$ (M^{-1} s^{-1})	δ Zr−H (ppm)	ϵ[a]
toluene-d_8	65(3)	7.48	2.4
diethyl ether-d_{10}	35(2)	7.30	4.3
tetrahydrofuran-d_8	17(5)	5.75	7.6
pyridine-d_5	no reaction	5.10	12.3

[a] Data taken from *CRC Handbook of Chemistry and Physics,* 67th ed.; CRC Press: Boca Raton, FL.

Table 3. Rate Constants for Reaction of $Cp^*_2ZrH_2$ (1) with Isobutene and *trans*-2-Butene as a Function of Temperature

temperature (K)	$k_{ins}^{isobutene} \times 10^4$ (M^{-1} s^{-1})	$k_{ins}^{trans-2-butene} \times 10^4$ (M^{-1} s^{-1})
220		4.2(1)
240		29(2)
250	3.3(1)	69(3)
263	8.5(1)	
275	19(3)	
296	65(3)	

Addition of either *cis*- or *trans*-2-butene to a toluene-d_8 solution of **1** affords the zirconocene *n*-butyl hydride complex $Cp^*_2Zr(CH_2CH_2CH_2CH_3)(H)$ (**8**) (eq 3). A zirconocene *sec*-butyl hydride intermediate has not been detected, even when the reaction is monitored at −90 °C. These results are contrary to those obtained with related zirconocene hydrido chloride[21a] and organoactinide complexes,[21b] where detection of the internal alkyl hydride complex has been achieved. Monitoring the reaction between **1** and *trans*-2-butene at low temperatures (T < 250 K) allows for measurement of the rate constant for insertion (Table 3). Likewise, the effect of temperature on the rate of isobutene insertion has also been determined, and those rate constants are also reported in Table 3. Attempts to measure similar rate constants for the insertion of *cis*-2-butene, propene, styrene, and 1-pentene have been unsuccessful due to the rapid rates of these reactions. Trisubstituted olefins such as 2-methyl-2-butene do not react with **1** over the course of several days at room temperature.

Isobutene, cyclopentene, styrene, and 1-pentene react with **2**, affording $Cp^*_2Hf(CH_2CHMe_2)(H)$ (**9**), $Cp^*_2Hf(cyclo\text{-}C_5H_9)(H)$ (**10**), $Cp^*_2Hf(CH_2CH_2C_6H_5)(H)$ (**11**), and $Cp^*_2Hf\{CH_2(CH_2)_3CH_3\}(H)$ (**12**). As with **1**, addition of

(19) Chirik, P. J.; Day, M. W.; Bercaw, J. E. *Organometallics* **1999**, *18*, 1873.

(20) Addition of 1 equiv of ethylene to $[(CpR_n)_2ZrH_2]_2$ results in clean formation of $(CpR_n)_2Zr(CH_2CH_3)(H)$. However, addition of excess ethylene results in reductive elimination of ethane and formation of the zirconocyclopentane. McAlister, D. R.; Erwin, D. R.; Bercaw, J. E. *J. Am. Chem. Soc.* **1978**, *100*, 5966.

(21) (a) Chirik, P. J.; Day, M. W.; Labinger, J. A.; Bercaw, J. E. *J. Am. Chem. Soc.* **1999**, *121*, 10308. (b) Lin, Z.; Marks, T. J. *J. Am. Chem. Soc.* **1990**, *112*, 5515.

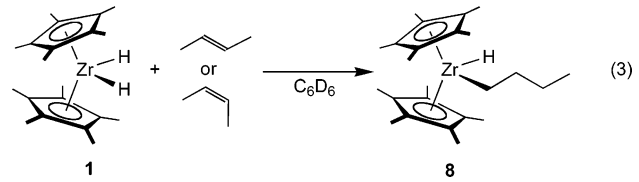

(3)

1 **8**

cis- or *trans*-2-butene to **2** immediately affords $Cp^*_2Hf(CH_2CH_2CH_2CH_3)(H)$ (**13**). In general, the rates of olefin insertion with **2** are slower than those for **1**. For example, the rate constant (23 °C) for isobutene insertion with **2** is 2.6×10^3 times slower than (the extrapolated value) for **1**. The slower rates of insertion for **2** permit quantitative determination of olefin insertion rate constants for this series of olefins. The rate constants for insertion of isobutene, *cis*-2-butene, and *trans*-2-butene have been determined over a range of temperatures (Table 4), permitting determinations of their activation parameters (Table 5). The rate constants for very fast insertions of 1-pentene and styrene for **2** have been measured at −43 °C. Using the experimentally determined rate constants and activation parameters, a quantitative comparison of the rates of insertion for each olefin studied has been obtained from extrapolation of the measured rates to a common temperature of −43 °C.

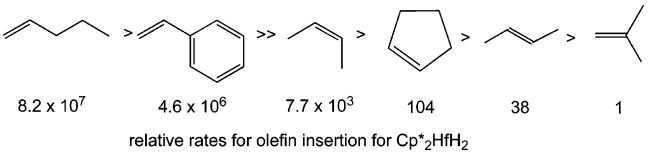

Isotope Effects on the Rate of Insertion. Preparation of $Cp^*_2ZrD_2$ (**1-*d*$_2$**) may be accomplished via addition of deuterium gas to a solution of **1** at −5 °C. At higher temperatures, incorporation of deuterium into the pentamethylcyclopentadienyl ligands is observed.[19] Mixing equimolar quantities of **1** and **1-*d*$_2$** in toluene-d_8 followed by addition of isobutene allows for measurement of the kinetic isotope effect for olefin insertion using the integration of the ^{1}H NMR isobutyl methine resonance versus the isobutyl methyl groups (both relative to an internal standard). From this analysis, a kinetic isotope effect, $k_H/k_D = 2.4$ (3), has been measured at 23 °C.

Linear Free Energy Relationship for the Insertion Reaction of α-Methylstyrene with 1. Addition of α-methylstyrene to a benzene-d_6 solution of **1** affords $Cp^*_2Zr\{CH_2CH(CH_3)C_6H_5\}(H)$ (**7**) (eq 4). The ^{1}H NMR spectrum of **7** displays two inequivalent Cp* rings and two diastereotopic C_α protons of the alkyl group. If the reaction reverses rapidly enough, equivalencing of the Cp* group and C_α protons would be expected. However, heating a sample of **7** does not result in coalescence of the Cp* or alkyl resonances, and eventually reductive elimination of alkane and decomposition of **7** is observed. Because reaction of **1** with α-methylstyrene is clean and proceeds at a convenient rate, electronic effects were probed by varying the *para* position of styrene. Addition of 4-fluoro-α-methylstyrene, 4-methyl-α-methylstyrene, 4-methoxy-α-methylstyrene, and 4-trifluoromethyl-α-methylstyrene to **1** affords $Cp^*_2Zr\{CH_2CH(CH_3)$-*p*-C_6H_4-F$\}(H)$ (**14**), $Cp^*_2Zr\{CH_2CH(CH_3)$-*p*-C_6H_4-$CH_3\}(H)$ (**15**), $Cp^*_2Zr\{CH_2CH(CH_3)$-*p*-C_6H_4-$OCH_3\}$(H) (**16**), and $Cp^*_2Zr\{CH_2CH(CH_3)$-*p*-C_6H_4-$CF_3\}(H)$ (**17**), respectively (eq 4). The rates of insertion for each reaction have been measured at 23 °C, and the observed rate constants are listed in Table 6. Construction of a Hammett plot reveals a better correlation to σ ($r^2 = 0.996$) than σ^+ ($r^2 = 0.667$), with $\rho = -0.46$ (1).[22]

Table 4. Rate Constants for Reaction of $Cp^*_2HfH_2$ (2) with Isobutene, *trans*-2-Butene, and *cis*-2-Butene as a Function of Temperature

temperature (K)	$k_{ins}^{isobutene} \times 10^6$ (M^{-1} s^{-1})	$k_{ins}^{trans-2-butene} \times 10^6$ (M^{-1} s^{-1})	$k_{ins}^{cis-2-butene} \times 10^6$ (M^{-1} s^{-1})
265			1200(100)
275			1900(400)
296	2.5(1)	62(5)	6200(200)
320		220(50)	
340		590(30)	
345	65(3)		
362	120(1)		

Table 5. Activation Parameters for Reaction of $Cp^*_2ZrH_2$ (1) and $Cp^*_2HfH_2$ (2) with Selected Olefins

metallocene dihydride	olefin	$\Delta S^‡$ (cal mol^{-1} K^{-1})	$\Delta H^‡$ (kcal mol^{-1})	$\Delta G^‡_{296K}$ (kcal mol^{-1})
$Cp^*_2ZrH_2$ (**1**)	isobutene	−38(3)	9.0(1)	20.2(1)
$Cp^*_2ZrH_2$ (**1**)	*trans*-2-butene	−29(3)	9.9(1)	18.5(1)
$Cp^*_2HfH_2$ (**2**)	isobutene	−43(10)	12.2(1)	24.9(2)
$Cp^*_2HfH_2$ (**2**)	*trans*-butene	−45(6)	9.7(1)	23.1(2)
$Cp^*_2HfH_2$ (**2**)	*cis*-2-butene	−48(8)	9.6(3)	23.7(3)
$Cp^*_2HfH_2$ (**2**)	cyclopentene	−43(8)	7.7(1)	20.4(5)

Table 6. Data for the Linear Free Energy Relationship for Insertion of *p*-Substituted α-Methylstyrenes with $Cp^*_2ZrH_2$ (1)

para substituent	$k_{ins} \times 10^5$ (M^{-1} s^{-1})	σ	σ^+
OCH_3	7.72(1)	−0.25	−0.78
CH_3	7.47(2)	−0.14	−0.30
H	6.92(1)	0	0
F	6.35(2)	0.15	−0.07
CF_3	5.45(2)	0.52	0.08

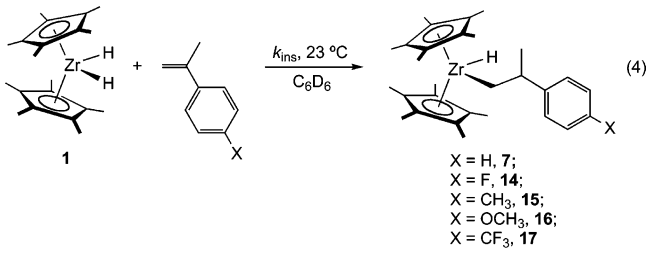

(4)

Effect of Cyclopentadienyl Substitution on the Rate of Isobutene Insertion. In addition to **1** and **2**, other monomeric zirconocene and hafnocene dihydrides have been reported.[19] Addition of isobutene to $Cp^*(\eta^5$-$C_5Me_4H)ZrH_2$ (**18**) results in quantitative formation of $Cp^*(\eta^5$-$C_5Me_4H)Zr(CH_2CHMe_2)(H)$ (**19**) with a rate constant of 3.3 (4) $\times 10^{-2}$ M^{-1} s^{-1} at −63 °C. Attempts to measure the rate of the reaction at higher temperatures have been unsuccessful due to the rapid rate of conversion. Extrapolating the isobutene insertion rate constant for **1** to −63 °C, using the experimentally determined activation parameters, yields a value of 8.7×10^{-6} M^{-1} s^{-1}; that is, **18** inserts isobutene 3800 times faster than does **1** at −63 °C.

(22) Values for σ and σ^+ were taken from: Isaacs, N. S. *Physical Organic Chemistry*; John Wiley and Sons: New York, 1986; p 131.

Table 7. Regiospecificity of Styrene Insertion for a Series of Zirconocene Dihydrides

zirconocene dihydride	1,2-product (%)	2,1-product (%)
$Cp^*_2ZrH_2$ (**1**)	100	0
$Cp^*\{(\eta^5\text{-}C_5H_3\text{-}1,3\text{-}(CMe_3)_2\}ZrH_2$ (**20**)	100	0
$\{(\eta^5\text{-}C_5H_3\text{-}1,3\text{-}(CMe_3)_2\}_2ZrH_2$ (**21**)	100	0
$Cp^*(\eta^5\text{-THI})ZrH_2$ (**31**)	60	40
$[(\eta^5\text{-}C_5Me_4H)_2ZrH_2]_2$ (**32**)	80	20
$Cp^*\{(\eta^5\text{-}C_5H_3\text{-}1,3\text{-}(CHMe_2)_2\}ZrH_2$ (**33**)	44	56
$[(\eta^5\text{-}C_5H_4\text{-}CMe_3)_2ZrH_2]_2$ (**30**)	0	100

Attempts to measure the rate of isobutene insertion for $Cp^*\{\eta^5\text{-}C_5H_3\text{-}1,3\text{-}(CMe_3)_2\}ZrH_2$ (**20**) and $\{\eta^5\text{-}C_5H_3\text{-}1,3\text{-}(CMe_3)_2\}_2ZrH_2$ (**21**) have been unsuccessful, as the rates of insertion are too fast to be measured by low-temperature NMR techniques. A rate constant of 5.1 (2) $\times 10^{-3}$ M^{-1} s^{-1} at 23 °C has been measured for the reaction of $Cp^*(\eta^5\text{-}C_5Me_4\text{-}CH_2CH_3)ZrH_2$ (**22**) with isobutene affording $Cp^*(\eta^5\text{-}C_5Me_4\text{-}CH_2CH_3)Zr(CH_2CHMe_2)$-(H) (**23**), approximately half the rate for the insertion of isobutene with **1**.

Preparation of $Cp^*\{\eta^5\text{-}C_5H_3\text{-}1,3\text{-}(CMe_3)_2\}HfH_2$ (**24**) has been accomplished via addition of *n*-BuLi to Cp^*-$\{\eta^5\text{-}C_5H_3\text{-}1,3\text{-}(CMe_3)_2\}HfCl_2$ under an atmosphere of H_2 as reported for **2**.[23] Reaction of **24** with isobutene results in clean formation of $Cp^*\{\eta^5\text{-}C_5H_3\text{-}1,3\text{-}(CMe_3)_2\}Hf(CH_2$-$CHMe_2)(H)$ (**25**). Rate constants for isobutene insertion have been measured between −48 and −3 °C and yield activation parameters of $\Delta H^{\ddagger} = 11.8(1)$ kcal·mol and $\Delta S^{\ddagger} = -27(5)$ eu.

Effect of Cyclopentadienyl Substitution on the Regiospecficity of Styrene Insertion. The influence of cyclopentadienyl substitution on the regiospecificity of olefin insertion has been examined for a series of zirconocene dihydride complexes. Reaction of **1** with styrene in benzene-d_6 results in clean formation of Cp^*_2-$Zr(CH_2CH_2C_6H_5)(H)$ (**26**), arising from the 1,2-insertion of the carbon−carbon double bond of the olefin (eq 5). Likewise, reaction of styrene with **20** and **21** affords solely primary insertion products, $Cp^*\{\eta^5\text{-}C_5H_3\text{-}(CMe_3)_2\}$-$Zr(CH_2CH_2C_6H_5)(H)$ (**27**) and $\{\eta^5\text{-}C_5H_3\text{-}(CMe_3)_2\}_2Zr$-$(CH_2CH_2C_6H_5)(H)$ (**28**), respectively (Table 7). Reaction of the less substituted zirconocene dihydride, $[Cp^*(\eta^5$-$C_5H_4\text{-}CMe_3)ZrH_2]_2$ (**30**), with styrene yields only the secondary insertion product, $Cp^*(\eta^5\text{-}C_5H_4\text{-}CMe_3)Zr\{CH$-$(CH_3)C_6H_5\}(H)$, as a 1:1 mixture of diastereomers. Confirmation of the regioselectivity of these reactions has been assayed via addition of CH_3OD to a benzene solution of the zirconocene phenethyl hydride. The resulting ethylbenzenes have been analyzed by $^2H\{^1H\}$ NMR spectroscopy, and the signals of 1-deutero-ethylbenzene and 2-deutero-ethylbenzene determined by integration versus an internal standard. Addition of styrene to $[Cp^*(THI)ZrH_2]_2$ (**31**) (THI = tetrahydroindenyl), $[(\eta^5\text{-}C_5Me_4H)_2ZrH_2]_2$ (**32**), and $Cp^*\{\eta^5\text{-}C_5H_3\text{-}1,3$-$(CHMe_2)_2\}ZrH_2$ (**33**) results in a mixture of regioisomers, depending on the substitution of the metallocene (Table 7). For **31** and **33** the 2,1-insertion products are formed as a ca. 1:1 mixture of diastereomers.

***β*-H Elimination Promoted by Internal Alkynes.** Reaction of the zirconocene dihydride complexes with alkynes leads to a variety of products depending on the

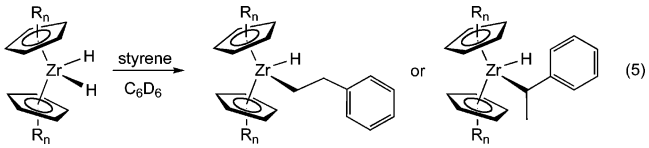

reaction conditions. Terminal alkynes such as 3,3-dimethyl-1-butyne produce mixtures of products arising from insertion of the alkyne, i.e., forming the alkenyl hydride complex, as well as those arising from σ bond metathesis with a Zr−H, generating the alkynyl complex and H_2 (eq 6). Small internal alkynes such as 2-butyne undergo rearrangement to afford crotyl hydride complexes.[24] However, sterically demanding, internal alkynes such as 4,4-dimethyl-2-pentyne (**37**) react with the series of zirconocene dihydrides to yield solely the insertion product, $(CpR_n)_2Zr\{C(CH_3)=CH(CMe_3)\}$-(H). In all cases examined, only one alkenyl hydride product is observed. Addition of CD_3OD to the series of zirconocene alkenyl hydride complexes and analysis of the resulting deuterated olefin by $^2H\{^1H\}$ NMR spectroscopy reveals that the zirconium center adds to the less hindered C_2 of the acetylene in each case (eq 7).

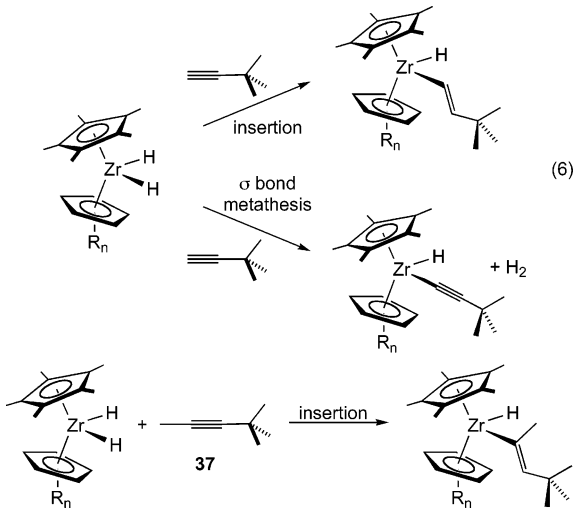

Reaction of **37** with the zirconocene alkyl hydride complexes also forms the alkenyl hydride complex and free olefin. These products are consistent with *β*-H elimination from the alkyl hydride liberating free olefin, and the zirconocene dihydride subsequently trapped by the acetylene in solution. Under the appropriate conditions (vide infra), this reaction allows for measurement of the rates of *β*-H elimination from a series of zirconocene alkyl hydride complexes.

A series of zirconocene isobutyl hydride complexes has been prepared from addition of isobutene to a benzene-d_6 solution of the zirconocene dihydride. In this manner, $Cp^*_2Zr(CH_2CHMe_2)(H)$ (**3**), $Cp^*(\eta^5\text{-}C_5Me_4H)Zr(CH_2$-$CHMe_2)(H)$ (**19**), $Cp^*(\eta^5\text{-}C_5H_5)Zr(CH_2CHMe_2)(H)$ (**38**), $Cp^*(\eta^5\text{-}C_5H_4\text{-}CMe_3)Zr(CH_2CHMe_2)(H)$ (**39**), $Cp^*(THI)$-$Zr(CH_2CHMe_2)(H)$ (**40**), $Cp^*\{\eta^5\text{-}C_5H_2\text{-}1,3\text{-}(CHMe_2)_2\}Zr$-$(CH_2CHMe_2)(H)$ (**41**), $Cp^*\{\eta^5\text{-}C_5H_3\text{-}1,3\text{-}(CMe_3)_2\}Zr(CH_2$-$CHMe_2)(H)$ (**42**), and $(\eta^5\text{-}C_5Me_4H)_2Zr(CH_2CHMe_2)(H)$ (**43**) have been prepared.

The observed rate constants for reaction of **19** and **38**−**43** with 4,4-dimethyl-2-pentyne (**37**) have been

(23) Roddick, D. M.; Fryzuk, M. D.; Seidler, P. F.; Hillhouse, G. L.; Bercaw, J. E. *Organometallics* **1985**, *4*, 97.

(24) McDade, C.; Bercaw, J. E. *J. Organomet. Chem.* **1985**, *279*, 281.

Table 8. Observed First-Order Rate Constants for the Reaction of Zirconocene Isobutyl Hydride Complexes with 4,4-Dimethyl-2-pentyne (37)

zirconocene isobutyl hydride	[**37**] (M)	$k_{obs} \times 10^6$ (s^{-1}) 2 °C	$k_{obs} \times 10^5$ (s^{-1}) 23 °C
$Cp^*_2Zr(CH_2CHMe_2)H$ (**3**)	0.244[a]	2.8(4)	
	0.650[a]	2.5(6)	
	1.10[a]	3.1(5)	
$Cp^*(\eta^5\text{-}C_5Me_4H)Zr(CH_2CHMe_2)H$ (**19**)	0.244		1.34(5)
	1.05		1.23(3)
	2.44		1.46(7)
$Cp^*CpZr(CH_2CHMe_2)H$ (**38**)	0.244	1060(20)	
	0.672	1120(50)	
	0.244	1030(40)	
$Cp^*(\eta^5\text{-}C_5H_4\text{-}CMe_3)Zr(CH_2CHMe_2)H$ (**39**)	0.244	335(4)	
	1.37	340(5)	
	4.88	382(9)	
$Cp^*(THI)Zr(CH_2CHMe_2)H$ (**40**)	0.152		108(2)
	0.908		108(4)
	1.32		107(3)
$Cp^*\{\eta^5\text{-}C_5H_3\text{-}1,3\text{-}(CHMe_2)_2\}Zr(CH_2CHMe_2)H$ (**41**)	1.22		284(6)
	0.244		298(8)
	1.22		270(5)
$Cp^*\{(\eta^5\text{-}C_5H_3\text{-}1,3\text{-}(CMe_3)_2\}Zr(CH_2CHMe_2)H$ (**42**)	0.122		33.5(5)
	1.37		34.0(2)
	4.88		38.2(8)
$(\eta^5\text{-}C_5Me_4H)_2Zr(CH_2CHMe_2)H$ (**43**)	0.061		54.4(2)
	0.244		54.3(5)
	0.976		52.6(3)

[a] 2-Butyne was used in place of **37**.

Scheme 1

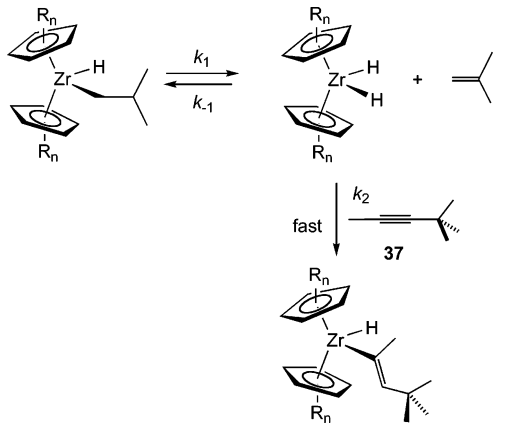

determined and found to be independent of the concentration of **37** over the range of 0.244 to 4.88 M (Table 8). For **3**, 2-butyne was used as the dihydride trap, since the reaction of **1** and **37** was not straightforward. Because the reverse of β-H elimination (k_{-1}) does not effectively compete with trapping (k_2) when several equivalents of alkyne are used, the rate of formation of the alkenyl product is effectively the rate of β-H elimination ($k_1 = k_{obs}$) (Scheme 1). Further evidence for the dissociative nature of the reaction on the acetylene concentration has been obtained through the use of two different acetylene traps. Reaction of **42** with 5 equiv of **37** or 2,2-dimethyl-1-butyne at −5 °C forms the alkenyl hydride complexes with observed rate constants of $3.3(4) \times 10^{-4}$ and $2.7(3) \times 10^{-4}$ s^{-1}, respectively. Activation parameters derived from the experimentally determined rate constants at various temperatures are given in Table 9. In all cases, the entropy of activation ($\Delta S^{\ddagger}$) is small, further supporting dissociative substitution of the alkyl by the alkenyl as shown in Scheme 1.

These data provide an interesting comparison of relative rates of β-H elimination for this series of zirconocene isobutyl hydrides as a function of ligand. Their values, normalized (or extrapolated) to that for **3** at 23 °C, are shown in Scheme 2.

Kinetic Isotope Effects for β-H Elimination. Preparation of isotopically labeled zirconocene isobutyl hydride complexes of the general formula $(CpR_n)_2Zr(CH_2CDMe_2)(D)$ has been accomplished via addition of isobutene to $(CpR_n)_2ZrD_2$.[21a] The isotopic purity of all of the compounds has been determined to be >95% based on ^1H and ^2H NMR spectroscopy. The rates of β-D elimination for $Cp^*(THI)Zr(CH_2CDMe_2)(D)$ (**40-*d*$_2$**), $Cp^*\{\eta^5\text{-}C_5H_3\text{-}1,3\text{-}(CHMe_2)_2\}Zr(CH_2CDMe_2)(D)$ (**41-*d*$_2$**), $Cp^*\{\eta^5\text{-}C_5H_3\text{-}1,3\text{-}(CMe_3)_2\}Zr(CH_2CDMe_2)(D)$ (**42-*d*$_2$**), $Cp^*(\eta^5\text{-}C_5Me_4H)Zr(CH_2CDMe_2)(D)$ (**19-*d*$_2$**), and $(\eta^5\text{-}C_5Me_4H)_2Zr(CH_2CDMe_2)(D)$ (**43-*d*$_2$**) have been determined at 23 °C by employing **37** as the trap for the intermediate zirconocene dideuteride. Comparison of these rate constants yields the kinetic isotope effect for β-H elimination for this series of isobutyl hydride complexes (k_H/k_D = 3.9 to 4.5) (Table 10).

Linear Free Energy Relationship for β-H Elimination. Reaction of **18** with *p*-substituted styrenes affords the phenethyl hydride complexes $Cp^*(\eta^5\text{-}C_5Me_4H)Zr(CH_2CH\text{-}p\text{-}C_6H_4\text{-}X)(H)$ (X = H, **44**; OCH_3, **45**; CH_3, **46**; CF_3, **47**) (Scheme 3). Reaction of each of the phenethyl hydride complexes with **37** as the dihydride trap affords rates of β-H elimination for each complex (Table 11). From these data a better linear free energy correlation to σ ($r^2 = 0.992$) than to σ^+ ($r^2 = 0.922$) is observed, displaying a ρ value of −1.80(5).

Rates of β-H Elimination with Different Alkyls. The effect of alkyl group on the rate of β-H elimination has been examined with a series of $Cp^*(\eta^5\text{-}C_5H_4\text{-}CMe_3)Zr(R)(H)$ complexes. Addition of the appropriate olefin to the hydride dimer **29** affords the zirconocene alkyl hydride complexes $Cp^*(\eta^5\text{-}C_5H_4\text{-}CMe_3)Zr(R)(H)$ (R = $CH_2CH_2CMe_3$, **48**; $CH_2(CH_2)_2CHMe_2$, **49**; $CH_2CH_2CH_2CH_3$, **50**; cyclopentyl, **51**). As with the zirconocene isobutyl hydride complexes, the rates of conversion of

Table 9. Activation Parameters for β-H Elimination for Zirconcene Isobutyl Hydride Complexes 38−42

zirconocene isobutyl hydride	$\Delta S^{\ddagger}$ (eu)	$\Delta H^{\ddagger}$ (kcal mol^{-1})	$\Delta G^{\ddagger}_{296K}$ (kcal mol^{-1})
Cp*CpZr(CH_2CHMe_2)H (**38**)	7.7(8)	21.9(4)	19.6(4)
Cp*(η^5-C_5H_4-CMe_3)Zr(CH_2CHMe_2)H (**39**)	−4.4(4)	18.8(6)	20.1(6)
Cp*(THI)Zr(CH_2CHMe_2)H (**40**)	3.1(8)	23.3(3)	21.3(4)
Cp*{η^5-C_5H_3-1,3-($CHMe_2$)$_2$}Zr(CH_2CHMe_2)H (**41**)	−4.1(9)	19.6(7)	20.8(8)
Cp*{(η^5-C_5H_3-1,3-(CMe_3)$_2$}Zr(CH_2CHMe_2)H (**42**)	−5.2(1)	20.5(3)	22.0(3)

Scheme 2

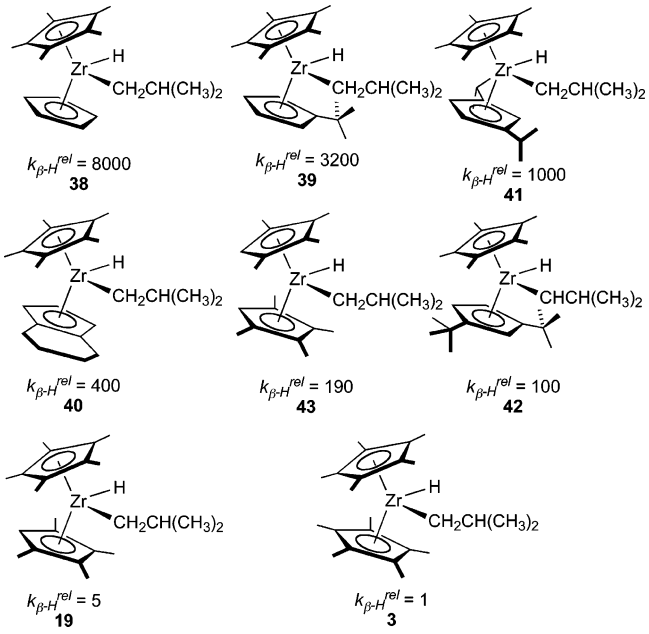

the alkyl to alkenyl (Table 12) are independent of the concentration of 4,4-dimethyl-2-pentyne (**37**); hence $k_{obs} = k_1 = k_{\beta-H}$.

Because the steric effects for β-H elimination for Cp*-(η^5-C_5H_4-CMe_3)Zr(R)(H) were much smaller than for olefin insertion with **2**, we wished to examine the effect of ancillary ligand substitution on the relative rates of β-H elimination for a series of *n*-butyl and isobutyl hydrides to establish whether insertion is more sensitive to steric effects more generally. The observed rate constants for these reactions are contained in Table 13. From these data, a general trend is observed: more substituted metallocenes have a ratio of β-H elimination rate constants ($k_{\beta-H}{}^{n-Bu}/k_{\beta-H}{}^{i-Bu}$) greater than 1, whereas less sterically hindered metallocenes have $k_{\beta-H}{}^{n-Bu}/k_{\beta-H}{}^{i-Bu}$ less than 1, implying that electronic effects (slightly) favor β-H elimination from isobutyl, but steric effects override this preference with the more crowded Cp*(η^5-C_5Me_4H)Zr(R)H.

Relative Ground-State Energies of Zirconocene Alkyl Hydride Complexes. Addition of 5 equiv of 1-butene to the series of zirconocene isobutyl hydride complexes results in formation of an equilibrium mixture of the zirconocene isobutyl hydride and the zirconocene *n*-butyl hydride complexes along with the free olefins (eq 8). Likewise, the equilibrium may be approached from addition of isobutene to the zirconocene *n*-butyl hydride complexes. The experimentally determined equilibrium constants and the corresponding free energy changes for these reactions are reported in Table 14.

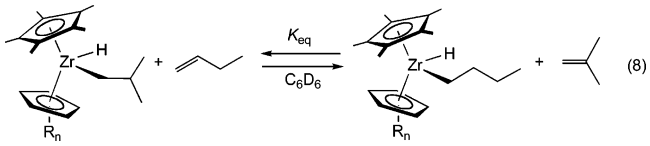

(8)

Discussion

Olefin Insertion for $(CpR_n)_2MH_2$ (M = Zr, Hf). The metallocene dihydride complexes $(CpR_n)_2MH_2$ (M = Zr, Hf) undergo facile reaction with unhindered α-olefins and internal olefins, affording the corresponding alkyl hydride complexes $(CpR_n)_2M(R')(H)$. On the basis of kinetic measurements of olefin insertion, conveniently measured using ^{1}H NMR spectroscopy, we have been able to elucidate the mechanism of olefin insertion into neutral, d^0 metallocene dihydride complexes. These experiments reveal the influence of olefin and cyclopentadienyl sterics on the rates of olefin insertion. The mechanistic sequence that is consistent with our evidence is shown in Scheme 4. The reaction proceeds via reversible coordination of the alkene followed by insertion through the normal four-centered transition structure. Although the geometry of the olefin dihydride adduct is unknown, we propose that olefin insertion takes place when the olefin occupies the lateral position (i.e., *cis* to only one zirconium hydride), based on preliminary density functional theory calculations with ethylene and Cp_2ZrH_2.[25] Reaction of isobutene with an equimolar mixture of $Cp^*_2ZrH_2$ and $Cp^*_2ZrD_2$ indicates a kinetic isotope effect of 2.4(3) at 23 °C. This value is indicative of a normal, primary isotope effect and is consistent with a pre-equilibrium involving rapid coordination and dissociation of olefin, followed by rate-determining hydride transfer. A similar kinetic profile has been proposed for reactions of olefins with $Cp^*_2M(OR)(H)$ (M = Th, U), where primary kinetic isotope effects of 1.4(1) and 1.3(2) have been measured for the insertion of cyclohexene and 1-hexene at 60 °C.[21b] These conclusions regarding rapid, reversible olefin binding with rate-determining insertion into the Zr−H bond are also in accord with reversible olefin binding and rate-limiting insertion into M−C bonds required to explain the secondary deuterium isotope effects that support α-agostic assistance for (1) hydrocyclization of α,ω-dienes by scandocene hydrides,[26] (2) hydrodimerization of 1-hexene by zirconocenium catalysts,[27] (3) the isotope effect on propylene chain propagation reported by Brintzinger and co-workers,[28] and (4) chain propagation

(25) Brandow, C. G.; Bercaw, J. E. Unpublished results.
(26) Piers, W. E.; Bercaw, J. E. *J. Am. Chem. Soc.* **1990**, *112*, 9406.
(27) Krauledat, H.; Brintzinger, H. H. *Angew. Chem., Int. Ed. Engl.* **1990**, *29*, 1412.
(28) LeClerc, M. K.; Brintzinger, H. H. *J. Am. Chem. Soc.* **1995**, *117*, 1651.

Table 10. Kinetic Isotope Effects for β-H Elimination for Isobutyl Hydride Complexes 19 and 40−43 at 23 °C

zirconocene isobutyl hydride	k_H (s^{-1})	k_D (s^{-1})	k_H/k_D
Cp*(η^5-C_5Me_4H)Zr(CH_2CDMe_2)D (**19-*d*$_2$**)	$1.34(9) \times 10^{-5}$	$3.29(12) \times 10^{-6}$	4.1(3)
Cp*(THI)Zr(CH_2CDMe_2)D (**40-*d*$_2$**)	$1.06(6) \times 10^{-3}$	$2.64(1) \times 10^{-4}$	4.1(2)
Cp*{η^5-C_5H_3-1,3-($CHMe_2$)$_2$}Zr(CH_2CDMe_2)D (**41-*d*$_2$**)	$2.8(8) \times 10^{-3}$	$7.10(7) \times 10^{-4}$	3.9(3)
Cp*{(η^5-C_5H_3-1,3-(CMe_3)$_2$}Zr(CH_2CDMe_2)D (**42-*d*$_2$**)	$3.52(9) \times 10^{-4}$	$7.81(10) \times 10^{-5}$	4.5(1)
(η^5-C_5Me_4H)$_2$Zr(CH_2CDMe_2)D (**43-*d*$_2$**)	$5.38(6) \times 10^{-4}$	$1.34(8) \times 10^{-4}$	4.0(2)

Scheme 3

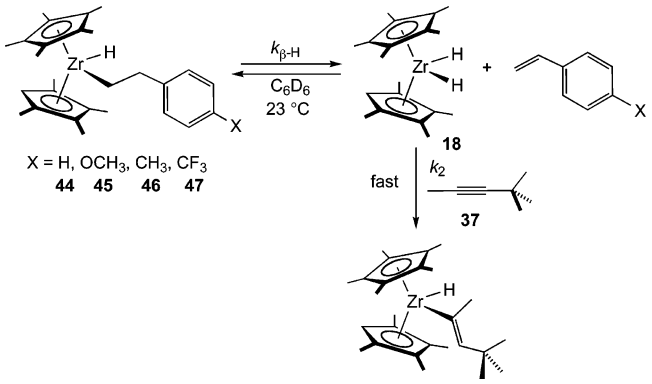

Table 11. Linear Free Energy Relationship Data for Phenethyl Complexes 44−47, Cp*(C_5Me_4H)Zr(CH_2CH_2-*p*-C_6H_5-X)(H)

phenethyl substituent	$k_{-H} \times 10^4$ (s^{-1}) 23 °C	σ	σ^+
X = CF_3 (**47**)	2.04(15)	0.53	0.08
X = H (**44**)	4.87(9)	0	0
X = CH_3 (**46**)	6.94(14)	−0.14	−0.30
X = OCH_3 (**45**)	8.53(6)	−0.25	−0.78

in 1-hexene polymerization as established by Landis and co-workers using heavy atom kinetic isotope effects.[29] If insertion into a Zr−H bond is slower than olefin binding or loss for 16-electron Cp*$_2$ZrH_2, then one might reasonably assume that insertion into a M−R bond (M = Sc, Zr; R = alkyl, polymeryl) would also be slower for 14-electron Cp_2Sc-R(olefin) or 16-electron [Cp_2Zr-R(solvento)]$^+$, given the universally slower olefin insertion into M−C versus M−H.

While there is not a large effect of solvent on the rate of isobutene insertion, the reaction proceeds more rapidly in solvents with lower dielectric constants than in those that have higher donicity (Table 2). This decrease appears to correlate with the chemical shift of the zirconium hydride. It has been shown previously that the ^{1}H NMR chemical shift of a group 4 metallocene hydride resonance may be used as a measure of electronic and coordinative unsaturation.[30] For the 16-electron dihydride complex Cp*$_2$ZrH_2 (**1**), the zirconium hydride resonance appears at 7.48 ppm (toluene-d_8), substantially downfield from 0.55 and 1.07 ppm observed for the 18-electron complexes Cp*$_2$ZrH_2(PF_3) and Cp*$_2$ZrH_2(CO) (both in toluene-d_8).[31] In donor solvents such as THF-d_8, the zirconocene hydride resonance for **1** shifts to 5.75 ppm, possibly indicating a buildup of significant amounts of the formally 18-electron solvento complex, although separate NMR signals for **1** and **1**-*solvento* are not observed, and low-temperature NMR experiments have not been attempted. If significant concentrations of 18-electon **1**-*solvento* do, in fact, form in the more polar solvents, olefin coordination would be impeded. A similar solvent effect has been noted in the related organoactinide complexes, Cp*$_2$M(OR)(H) (M = Th, U), for which $k_{THF}/k_{toluene} = 0.59$.[21b]

Addition of *para*-substituted α-methylstyrenes, *p*-CH_2=C(CH_3)(C_6H_4-X) (X = H, CH_3, CF_3, OCH_3), to **1** affords the zirconocene alkyl hydrides **7** and **14**−**17**. A better linear free energy correlation of the observed rate constants is obtained with the Hammett constant σ (vis-à-vis σ^+) with $\rho = -0.46(1)$. Better correlation to σ has also been observed with permethylniobocene and permethyltantalocene styrene hydride complexes, where X-ray crystal structures indicate that the p orbital of the β-carbon and the π system of the phenyl ring are twisted out of resonance by approximately 30°. In the transition state for insertion the pseudo-five-coordinate carbon does not allow for full overlap of the β-carbon and the phenyl ring π system.[8b] The relatively small, negative ρ value of −0.46(1) is indicative of a cyclic transition state with little charge separation, with only a slight positive charge development at the β-carbon of the coordinated olefin, thus implicating transfer of hydrogen as closer to H$^\bullet$ than H$^-$. Also consistent with these findings are the highly negative entropies of activation (−30 to −48 eu) indicating a highly ordered transition structure for olefin insertion. Therefore, the transition-state model developed for the niobocene and tantalocene olefin hydride complexes may be extended to Cp*$_2$MH_2.

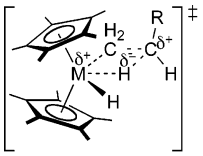

(M = Zr, Hf) $|\delta|_{ins}$ small

The effect of olefin substitution on the rate of insertion has also been examined with **1** and **2**. Not surprising is the observed decrease in rate of insertion for more hindered olefins (eq 2); however, the effect for **1** is rather small, at least for the range of olefins examined (Table 1). Placing a methyl at either the 3 or 4 position of the olefin has little effect on the rate of insertion for 2-methyl-substituted olefins. For example, the rate of isobutene insertion is approximately 10 times faster than that for 2,4-dimethyl-1-pentene. On the other hand, further increasing the substitution of the 4-position of olefin, as in the case of 2,4,4-trimethyl-1-pentene, produces no reaction with the zirconium hydride. Attempts to hydrogenate this olefin in the presence of **1**

(29) Landis, C. R.; Rosaaen, K. A.; Uddin, J. *J. Am. Chem. Soc.* **2002**, *122*, 10358.

(30) (a) Bercaw, J. E. In *Transition Metal Hydrides*; Advances in Chemistry Series 167; 1978; Chapter 10, p 136. (b) Hillhouse, G. L.; Bulls, A. R.; Santarsiero, B. D.; Bercaw, J. E. *Organometallics* **1988**, *7*, 1309.

(31) Manriquez, J. M.; McAlister, D. R.; Sanner, R. D.; Bercaw, J. E. *J. Am. Chem. Soc.* **1978**, *100*, 2716.

Table 12. Rates of β-H Elimination as a Function of Alkyl Ligand for Cp*(η^5-C_5H_4-CMe_3)Zr(R)(H) Complexes 39 and 48−51 at 23 °C

alkyl group (R)	olefin released	$k_{-H} \times 10^4$ (s^{-1}) 23 °C	relative rate
R = $CH_2CH_2CMe_3$ (**48**)	3,3-dimethyl-1-butene	1.47(8)	1
R = $CH_2(CH_2)_2CHMe_2$ (**49**)	3-methyl-1-pentene	17.8(6)	12.1
R = $CH_2(CH_2)_2CH_3$ (**50**)	1-butene	18.3(5)	12.4
R = CH_2CHMe_2 (**39**)	isobutene	90.6(6)	62
R = cyclopentyl (**51**)	cyclopentene	1000(25)	680

Table 13. Comparison of the Rates at 23 °C for β-H Elimination for a Series of Zirconocene *n*-Butyl and Isobutyl Hydride Complexes

zirconocene butyl hydride (R = $CH_2CH_2CH_2CH_3$, CH_2CHMe_2)	$k_{-H}{}^{n\text{-Bu}}$ (s^{-1})	$k_{-H}{}^{i\text{-Bu}}$ (s^{-1})	$k_{-H}{}^{n\text{-Bu}}$:$k_{-H}{}^{i\text{-Bu}}$
Cp*(η^5-C_5Me_4H)Zr(R)H	$7.85(2) \times 10^{-5}$	$1.34(9) \times 10^{-5}$	5.86
Cp*{(η^5-C_5H_3-1,3-$(CMe_3)_2$}Zr(R)H	$3.35(9) \times 10^{-4}$	$3.5(2) \times 10^{-4}$	0.96
Cp*(THI)Zr(R)H	$9.28(1) \times 10^{-4}$	$1.06(6) \times 10^{-3}$	0.875
Cp*{η^5-C_5H_3-1,3-$(CHMe_2)_2$}Zr(R)H	$9.88(2) \times 10^{-4}$	$2.8(8) \times 10^{-3}$	0.357
Cp*(η^5-C_5H_4-CMe_3)Zr(R)H	$1.83(5) \times 10^{-3}$	$9.06(6) \times 10^{-3}$	0.201

Table 14. Equilibrium Constants and Free Energy Data for the Isobutyl Hydride:*n*-Butyl Hydride Equilibrium (eq 8)

zirconocene butyl hydride (R = $CH_2CH_2CH_2CH_3$, CH_2CHMe_2)	$K_{eq}{}^{296\ K}$ (M^{-1})	$\Delta G^{\ddagger}_{296K}$ (kcal mol^{-1})
Cp*$_2$Zr(R)H	51(3)	−2.3(2)
Cp*(η^5-C_5Me_4H)Zr(R)H	43(3)	−2.1(2)
Cp*{η^5-C_5H_3-1,3-$(CMe_3)_2$}Zr(R)H	25(4)	−1.9(2)
Cp*{η^5-C_5H_3-1,3-$(CHMe_2)_2$}Zr(R)H	16(2)	−1.7(1)
Cp*(η^5-THI)Zr(R)H	9.6(3)	−1.3(1)
Cp*(η^5-C_5H_4-CMe_3)Zr(R)H	9.1(4)	−1.3(1)

Scheme 4

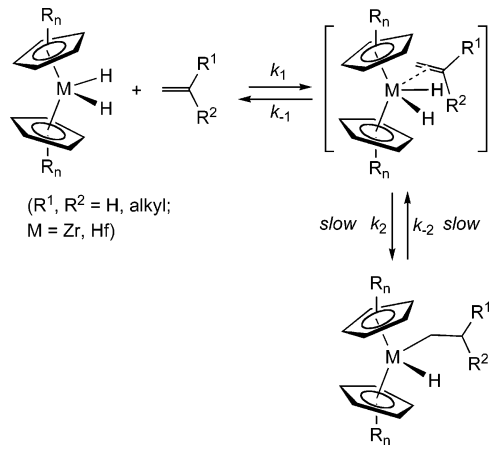

also results in no reaction, demonstrating its inability to insert into the zirconium hydride bond under normal conditions. Changing the steric disposition of the olefin (e.g., *cis*-2-butene versus isobutene) has a dramatic impact on the rate of insertion with **1** and Cp*$_2$$HfH_2$ (**2**). Internal olefins such as *cis*- and *trans*-2-butene insert much faster than 1,1-disubstituted olefins. For both metallocenes, the rate of *cis*-2-butene insertion is faster than for *trans*; with **2** the *cis* isomer inserts approximately 100 times faster than *trans*. The reason for the faster insertion of the *cis* isomer is not clear, but this preference seems general, even for late transition metal hydrides.[32] The very large difference observed for **2** likely reflects less steric hindrance in the transition state for insertion, *cis*-2-butene having its substituents placed on one side only.

The rate of insertion for α-olefins (e.g., 1-pentene, styrene) with **2** is approximately 10^8 times faster than that for 1,1-disubstituted olefins at −43 °C. Unfavorable steric interactions between the more substituted 1,1-disubstituted olefins and the bulky pentamethylcyclopentadienyl ligands are almost certainly responsible for the dramatic difference in rates. These results are in accord with previous studies that demonstrate α-olefins undergo hydrozirconation more rapidly than 1,1-disubstituted olefins.[33] Similar observations have been made in metallocene-catalyzed olefin polymerization, where it is commonly found that α-olefins undergo insertion at a much greater rate than 1,1-disubstituted olefins.[34] Casey[35] has estimated the differences in binding energies for mono- and disubstituted alkenes using model yttrocene olefin alkyl chelate complexes. Using 2,5-dimethyltetrahydrofuran as a competing ligand, the enthalpy for olefin binding was found to be approximately 2.0 kcal·mol^{-1} stronger for the monosubstituted alkene complex as compared to the 1,1-disubstituted olefin chelate.

These results have special relevance to the chain epimerization mechanism proposed by Busico to account for the tacticity dependence on monomer concentration in metallocene-catalyzed isospecific olefin polymerization.[36] The change in olefin enantioface is accomplished via initial β-H elimination to a 1,1-disubstituted olefin hydride cation intermediate. A key feature of the mechanism involves in-plane olefin rotation about the π face of the coordinated alkene and a switch of Zr from one enantioface to the other, presumably via weak coordination to the σ framework. It is assumed that once the 1,1-disubstituted olefin is lost from the metal center and its solvent sphere, it cannot compete for reinsertion into Zr−H with the high concentration of propylene monomer present.[37] For **2** the observed much slower insertion of isobutene as compared with 1-pentene (a factor of 8×10^7) supports this assertion; the observed rate difference would not allow reinsertion of the

(32) Collman, J. P.; Hegedus, L. S.; Norton, J. R.; Finke, R. G. *Principles and Applications of Organotransition Metal Chemistry*; University Science Books: Mill Valley, CA, 1987.

(33) Labinger, J. A. In *Comprehensive Organic Synthesis*; Trost, B. M., Fleming, I., Eds.; Pergamon Press: Oxford, 1991; Chapter 3.9.

(34) Busico, V.; Cippullo, R. *J. Am. Chem. Soc.* **1994**, *116*, 9329.

(35) Casey, C. P.; Fisher Klein, J.; Fagan, M. A. *J. Am. Chem. Soc.* **2000**, *122*, 4320.

(36) Busico, V.; Caporaso, L.; Cippulo, R.; Landriani, L.; Angelini, G.; Margonelli, A.; Segre, A. L. *J. Am. Chem. Soc.* **1996**, *118*, 2105.

(37) Yoder, J. C.; Bercaw, J. E. *J. Am. Chem. Soc.* **2002**, *124*, 2548.

vinylidene end group of the polymer chain, especially in the presence of such a large excess of α-olefin.

Cyclopentadienyl ligand substitution may have a very striking effect on the rate of olefin insertion. Comparing the rates of isobutene insertion for **1** and **18** at −63 °C reveals a 3.8×10^3-fold rate enhancement for the latter! Such a large rate increase on replacing with hydrogen only one of the 10 cyclopentadienyl methyl groups must indicate the transition state for isobutene insertion with **1** is very hindered. Similar effects are observed with Cp*(η^5-C_5H_3-1,3-$(CMe_3)_2$)ZrH_2 (**20**) and (η^5-C_5H_3-1,3-$(CMe_3)_2)_2ZrH_2$ (**21**), where in both cases the reduced steric disposition of ligand vis-à-vis **1** results in insertion rates that are too fast to measure with NMR techniques, even at −63 °C. On the other hand, the rate of isobutene insertion is not changed by replacement of one of the pentamethylcyclopentadienyl methyl groups with an ethyl group; isobutene inserts for **22** at about half the rate as for **1**.

Cyclopentadienyl substitution also has a significant effect on the regiospecificity of styrene insertion. More crowded metallocenes such as **1**, **18**, **20**, and **21** proceed with high regioselectivity, yielding solely the 1,2-insertion product. However, more open metallocenes, **31**, **32**, and **33**, form mixtures of both 1,2- and 2,1-insertion products, and in one case, **29**, only 2,1-insertion products are formed. From these results, it appears that in the absence of overriding steric effects, styrene prefers to insert in a 2,1-fashion, presumably due to electronic stabilization of the Zr−C bond by an α-phenyl substituent.[38]

The experimentally determined rate constants and resulting activation parameters allow for direct comparison of the insertion barrier for zirconium and hafnium (Table 5). For isobutene and *trans*-2-butene, the $\Delta G^{\ddagger}$ for insertion into a Zr−H bond is approximately 4 kcal·mol^{-1} lower than that for the corresponding Hf−H bond, corresponding to an approximate insertion rate ratio of 10^3. Similar differences in activity have been observed in a variety of zirconium and hafnium catalytic systems and may be attributed to the ground-state stabilization due to the greater Hf−H bond dissociation energy.

***β*-H Elimination for $(CpR_n)_2M(R')(H)$ (R, R′ = alkyl).** Zirconocene alkyl hydride complexes of the general formula $(CpR_n)_2Zr(R')(H)$ (R, R′ = alkyl) undergo facile (reversible) *β*-H elimination as determined by trapping with 4,4-dimethyl-2-pentyne (**37**). Because the rate of trapping is faster, even with only a few equivalents of **37** (Scheme 1), the rates of *β*-H elimination for a series of zirconocene isobutyl hydride complexes is readily established (Scheme 2). In general, more substituted metallocenes display slower rates of *β*-H elimination, although in comparison to olefin insertion, rates of *β*-H elimination are much less affected by ancillary ligand substitution. For example, comparing the [Cp^*_2Zr] system to the only slightly less hindered [Cp*(η^5-C_5Me_4H)Zr] system, insertion of isobutene with **18** is 3800 times faster than for **1**, whereas in the reverse reaction, *β*-H elimination for **19** is only 5 times faster than for **3**. Whereas the same unfavorable steric interactions are present in the transition state for both directions, steric interactions increase more dramatically as the reaction proceeds in the insertion direction, beginning with separated olefin and relatively uncrowded zirconocene dihydride. By contrast, in the *β*-H elimination direction the alkyl already possesses some unavoidable steric interactions with the cyclopentadienyl ligands that increase comparatively little in accessing the transition state.

Scheme 5

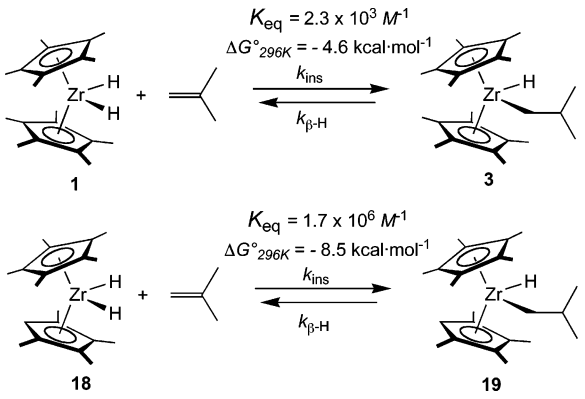

Because the rates of both olefin insertion and *β*-H elimination have been measured (or extrapolated from activation parameters) at 23 °C for the [Cp^*_2Zr] system as well as for the less hindered [Cp*(η^5-C_5Me_4H)Zr] system, the equilibrium constants for the addition of isobutene to the dihydrides can be computed (Scheme 5). Assuming a negative value for the reaction entropy ($\Delta S° = -20$ eu is assumed), the insertion of isobutene with **1** is rather exothermic, $\Delta H° \approx -10.5$ kcal·mol^{-1} and for **18** $\Delta H° \approx -14.4$ kcal·mol^{-1}.

Although it is difficult to confidently compare the bis(pentamethylcyclopentadienyl)hafnium system (for which we have relative insertion rates) to the (pentamethylcyclopentadienyl)(*tert*-butylcyclopentadienyl)zirconium system (for which we have relative rates of *β*-H elimination), the rate constants for *β*-H elimination (Table 12) appear to be influenced substantially less by the steric demands of the olefin, as compared to olefin insertion with $Cp^*_2HfH_2$ (**2**). Moreover, the $k_{\beta-H}$ values do not follow an obvious order; less hindered α-olefins are eliminated faster, yet the *n*-alkyl hydrides *β*-H eliminate 50−700 times *slower* than the cyclopentyl hydride. The latter order is opposite that for insertion; α-olefins such as 1-pentene undergo insertion with **2** approximately 10^6 times *faster* than cyclopentene. These data allow a rough comparison that indicates that the equilibrium between dihydride + olefin and the alkyl hydride ($k_{ins}/k_{\beta-H} = K_{eq}$) lies toward the *n*-alkyl hydride by several orders of magnitude (i.e., the equilibrium lies much more toward the *n*-pentyl hydride than it does toward cyclopentyl hydride).

Cyclopentadienyl steric effects on *β*-H elimination have also been observed for the polymerization of propylene with metallocene catalysts. Polypropylene produced from Cp_2ZrCl_2/MAO mixtures terminates primarily by *β*-H elimination, whereas the polyolefin generated from $Cp^*_2ZrCl_2$/MAO mixtures contains end groups arising from chain termination by *β*-methyl elimination. The increased preference for *β*-methyl elimination for the latter system is believed to be a

(38) Nelson, J. E.; Bercaw, J. E.; Labinger, J. A. *Organometallics* **1989**, *8*, 2404, and references therein.

Scheme 6

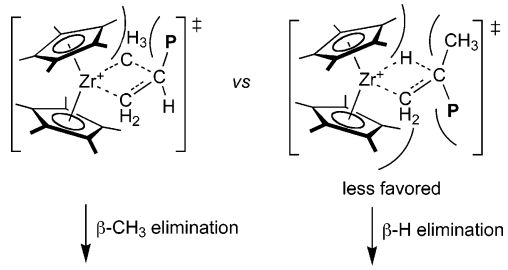

result of inhibition of β-H elimination by the sterically demanding pentamethylcyclopentadienyl rings (Scheme 6).[39]

The kinetic isotope effects for β-H elimination have been determined with a series of zirconocene isobutyl hydride complexes, $(CpR_n)_2Zr(CH_2CLMe_2)(L)$ (L = H or D). In all cases a normal, primary isotope effect has been observed (Table 10). These data suggest that β-H elimination proceeds via rate-determining C−H(D) bond cleavage followed by rapid dissociation of the coordinated olefin. The values obtained in this study (∼4) are somewhat larger than those measured for related systems. A primary kinetic isotope effect of 2.0 has been measured for β-H elimination in the scandium phenethyl complex $Cp^*_2ScCH_2CH_2C_6H_5$.[9] Likewise, a smaller kinetic isotope effect of 1.6 has been measured for the β-H elimination in the polymerization of propene with 2-d_1-propene with $[(Me_2Si)_2\{\eta^5\text{-}C_5H\text{-}3,5\text{-}(CHMe_2)_2\}(\eta^5\text{-}C_5H_2\text{-}4\text{-}CHMe_2)]ZrCl_2$/methyalumoxane mixtures.[40] The larger values for the alkyl hydrides in the current study may reflect a somewhat later transition state (more C−H bond breaking) for the less electrophilic, neutral group 4 metallocene derivatives.

The electronic effects on the rate of β-H elimination, probed with a series of *para*-substituted phenethyl hydride complexes, $Cp^*(\eta^5\text{-}C_5Me_4H)Zr(CH_2CH_2\text{-}p\text{-}C_6H^5\text{-}X)(H)$ (X = H, Me, OCH_3, CF_3), are also indicative of positive charge development in the transition structure ($\rho = -1.80(5)$). The magnitude of the effects is very similar to that found for β-H elimination for $Cp^*_2ScCH_2\text{-}CH_2\text{-}p\text{-}C_6H_4\text{-}X$ ($\rho = -1.87$).[9] Interestingly, here we have for comparison a measurement of the electronic effects in the olefin insertion direction ($\rho = -0.49$), substantially less than for the β-H elimination direction, once again suggesting that the transition state for the latter is comparatively late, with more charge developing in that direction. Given the exothermicity of olefin insertion (Scheme 5), such asymmetry is reasonable.

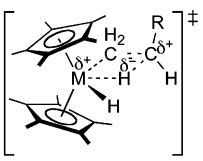

(M = Zr, Hf) $|\delta|_{\beta\text{-H elim}}$ moderate

Delineation of Ground- versus Transition-State Effects in β-H Elimination. Measurement of the barriers for β-H elimination as well as the free energy changes for equilibrating the zirconocene isobutyl hydride and *n*-butyl hydride presents a rare opportunity to differentiate the contributions of ground-state and transition-state effects for β-H elimination. The free energy change for eq 8 (Table 14) provides a basis for assessing the relative ground-state energies of the two zirconocene alkyl hydride complexes (Scheme 7). The change in free energy accompanying eq 8 is not the free energy difference between the isobutyl and *n*-butyl hydride complexes, but rather a composite of the relative zirconocene alkyl hydride ground states and the change in free energy for the isomerization of 1-butene to isobutene. Addition of the value[41] (+3.2 kcal·mol^{-1}) for the reverse of the latter to the free energy change for eq 8 yields the relative ground-state free energy differences ($\Delta G°_{296K}$(met)) for two zirconocene alkyl hydride complexes (Table 15). Note that these calculations allow ordering of the relative ground states of the *n*-butyl hydride as compared to the isobutyl hydride for a given ligand array, but do not allow comparison of the ground states of two alkyl hydride complexes with different cyclopentadienyl ligands.

Scheme 7

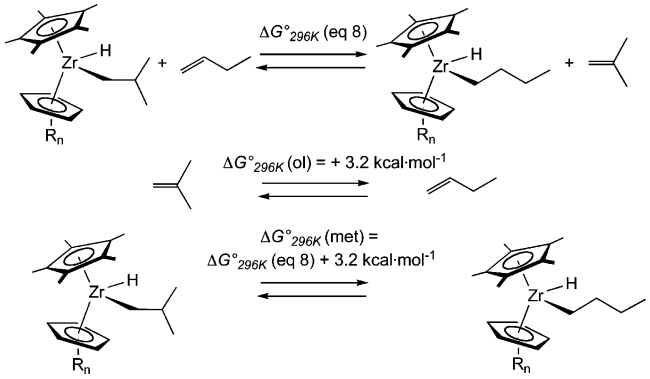

In all cases examined, the zirconocene isobutyl hydride is thermodynamically favored over the corresponding *n*-butyl hydride complex. In an attempt to understand the electronic contribution of this effect, the free energies of formation of isobutane and *n*-butane have been examined. At 23 °C, the branched alkane is favored by 1.10 kcal·mol^{-1} over the linear alkane,[41] in accord with the observed preference for the zirconocene. We have previously noted a fairly general correlation between metal−carbon and carbon−hydrogen bond strengths, allowing the relative strengths of M−C bonds to be predicted from the relative energies of the corresponding C−H bonds.[42] Accordingly, the $[Cp_2ZrH]$ moiety has a thermodynamic preference for the more stable alkyl and therefore prefers the isobutyl hydride over the *n*-butyl hydride by a predicted 1.10 kcal·mol^{-1}. Although electronic preferences favoring the isobutyl hydride are important, as it is favored over the *n*-butyl hydride for all, cyclopentadienyl ligand substitution does influence the position of the equilibrium. For less substituted zirconocenes such as $[Cp^*(\eta^5\text{-}C_5H_4\text{-}CMe_3)Zr]$ and [Cp*-(THI)Zr], the electronic contributions are apparent, as

(39) (a) Resconi, L.; Piemontesi, F.; Franciscono, G.; Abis, L.; Fiorani, T. *J. Am. Chem. Soc.* **1992**, *114*, 1025. (b) Horton, A. D. *Organometallics* **1996**, *15*, 2675. (c) Chirik, P. J.; Bercaw, J. E. *Organometallics* **2005**, *24*, 2789.

(40) Veghini, D.; Henling, L. M.; Burkhardt, T. J.; Bercaw, J. E. *J. Am. Chem. Soc.* **1999**, *121*, 564.

(41) Benson, S. W. *Thermochemical Kinetics*, 2nd ed.; Wiley and Sons: New York, 1976.

(42) (a) Bryndza, H. E.; Fong, L. K.; Paciello, R. A.; Tam, W.; Bercaw, J. E. *J. Am. Chem. Soc.* **1987**, *109*, 1444. (b) Labinger, J. A.; Bercaw, J. E. *Organometallics* **1988**, *7*, 926.

Table 15. Relative Ground-State Free Energies for Zirconocene Isobutyl and *n*-Butyl Hydride Complexes (see Scheme 7)

zirconocene butyl hydride (R = $CH_2CH_2CH_2CH_3$, CH_2CHMe_2)	$\Delta G^{\ddagger}_{296K}$(met) (kcal mol^{-1})	$\Delta G^{\ddagger}_{296K}$(met) − $\Delta G^{\ddagger}_{296K}$(alkane) (kcal mol^{-1})
$Cp^*_2Zr(R)H$	0.90 (2)	−0.2
$Cp^*(\eta^5\text{-}C_5Me_4H)Zr(R)H$	1.0 (2)	−0.1
$Cp^*\{\eta^5\text{-}C_5H_3\text{-}1,3\text{-}(CMe_3)_2\}Zr(R)H$	1.3 (2)	0.2
$Cp^*\{\eta^5\text{-}C_5H_3\text{-}1,3\text{-}(CHMe_2)_2\}Zr(R)H$	1.5 (1)	0.4
$Cp^*(\eta^5\text{-THI})Zr(R)H$	1.9 (1)	0.8
$Cp^*(\eta^5\text{-}C_5H_4\text{-}CMe_3)Zr(R)H$	1.9 (1)	0.8

Table 16. Relative Ground-State Energies, *β*-H Activation Free Energies, and Calculated *β*-H Transition-State (TS) Free Energy Differences for Zirconocene Isobutyl and *n*-Butyl Hydride Complexes

zirconocene butyl hydride (R = $CH_2CH_2CH_2CH_3$ & CH_2CHMe_2)	$\Delta G^{\ddagger}_{296K}$(met) (kcal mol^{-1})	$\Delta G^{\ddagger}_{\beta-H}{}^{isobutyl}$ (kcal mol^{-1})	$\Delta G^{\ddagger}_{\beta-H}{}^{n-butyl}$ (kcal mol^{-1})	$TS^{n-butyl} - TS_{\beta-H}{}^{isobutyl}$ (kcal mol^{-1})
$Cp^*(\eta^5\text{-}C_5Me_4H)Zr(R)H$	1.0 (2)	23.9	22.9	0
$Cp^*\{\eta^5\text{-}C_5H_3\text{-}1,3\text{-}(CMe_3)_2\}Zr(R)H$	1.3 (2)	22.0	22.0	1.3
$Cp^*\{\eta^5\text{-}C_5H_3\text{-}1,3\text{-}(CHMe_2)_2\}Zr(R)H$	1.5 (1)	21.3	21.4	1.6
Cp*(THI)Zr(R)H	1.9 (1)	20.8	21.4	2.5
$Cp^*(\eta^5\text{-}C_5H_4\text{-}CMe_3)Zr(R)H$	1.9 (1)	20.1	21.0	2.8

the free energy difference exceeds that for the alkanes.[43] For more crowded members of the series, [Cp^*_2Zr] and [$Cp^*(\eta^5\text{-}C_5Me_4H)Zr$], steric destabilization of the isobutyl hydride complex makes the isobutyl hydride preference less than for the alkanes. The energetics of this steric contribution from such estimates spans (only) 1.0 kcal·mol^{-1}.

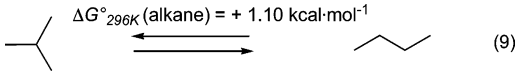

(9)

Grubbs[44] has found similar behavior for alkyl-substituted titanacyclobutanes, where the more stable titanocycle is derived from the more stable olefin, presumably a result of the structural features of the metallacycle. Likewise, Wolczanski has found a similar correlation between metal−carbon bond strengths and carbon−hydrogen bond strengths in the equilibration of tris-amido zirconium alkyl complexes.[45]

From the experimentally determined rates of *β*-H elimination and the relative ground-state energies of the zirconocene isobutyl and *n*-butyl hydrides, the relative transition-state energies for the *β*-H elimination reaction can be quantitatively ordered. The activation free energy may be calculated for each *β*-H elimination reaction from the rate constant. Subtraction of the relative ground-state contributions for each of the zirconocene alkyl hydrides affords the relative transition-state energies for both zirconocene alkyl hydrides for a given ligand array. The relative ground-state, activation, and transition-state energies are contained in Table 16.

On the basis of electronic considerations and the model established for the transition state for *β*-H elimination (vide supra), the free energy of the transition state for a zirconocene isobutyl hydride would be expected to be lower than that for the corresponding zirconocene *n*-butyl hydride, because the more substituted alkyl would better stabilize the developing positive charge on the *β*-carbon. On the other hand, considering steric considerations, the *β*-H elimination transition state for the zirconocene *n*-butyl hydride would be favored due to decreased steric interactions with the bulkier cyclopentadienyl ligands.

The experimentally determined transition state energy differences indicate that for the sterically crowded metallocene [$Cp^*(\eta^5\text{-}C_5Me_4H)Zr$] these effects almost exactly cancel, and as a result, the isobutyl and *n*-butyl hydride transition states are of equal energy (Figure 1). Thus, the faster rate of *β*-H elimination for $Cp^*(\eta^5\text{-}C_5Me_4H)Zr(CH_2CH_2CH_2CH_3)(H)$ is a result of electronic stabilization of the $Cp^*(\eta^5\text{-}C_5Me_4H)Zr(CH_2CHMe_2)(H)$ in the ground state. For less substituted metallocenes, the electronically favored isobutyl hydride transition state becomes more and more favored over the sterically preferred *n*-butyl hydride transition state. This effect increases with decreasing substitution on the metallocene, and as a result, the least crowded metallocene, [$Cp^*(\eta^5\text{-}C_5H_4\text{-}CMe_3)Zr$], displays the largest transition-state energy difference.

From these data, the relative rates of *β*-H elimination can be rationalized (Table 13). For less crowded metallocenes such as [$Cp^*(\eta^5\text{-}C_5H_4\text{-}CMe_3)Zr$] and [$Cp^*\{\eta^5\text{-}C_5H_3\text{-}1,3\text{-}(CHMe_2)_2\}Zr$], the electronic stabilization of the isobutyl hydride transition state overcomes its favored ground-state stabilization relative to the *n*-butyl hydride, and as a result, faster rates of isobutyl hydride *β*-H elimination are observed. For intermediate metallocenes, these effects are similar, although the transition-state effects dominate and faster isobutyl hydride *β*-H elimination rates are still observed. Only in the most crowded member of the series, [$Cp^*(\eta^5\text{-}C_5Me_4H)Zr$], are the transition-state effects overcome by ground-state effects.

From these studies, a moderately comprehensive description of the *β*-H elimination reaction has been established. The reaction proceeds via rate-determining C−H bond scission via a four-centered transition-state structure that has a modest buildup of positive charge on the *β*-carbon, resulting in transfer of $H^{\delta-}$ to the metal center. The rate of *β*-H elimination is influenced by the structure of the ancillary ligation. For a given alkyl, the rate of *β*-H elimination decreases with increasing cyclopentadienyl ligand substitution. When considering

(43) Although a correlation exists between M−C and C−H bond strengths, it is not absolute, and as a result, differences in M−C bond dissociation energies often exceed the differences in the corresponding C−H bond strengths.

(44) Straus, D. A.; Grubbs, R. H. *Organometallics* **1982**, *1*, 1658.

(45) Schaller, C. P.; Cummins, C. C.; Wolczanski, P. T. *J. Am. Chem. Soc.* **1996**, *118*, 591.

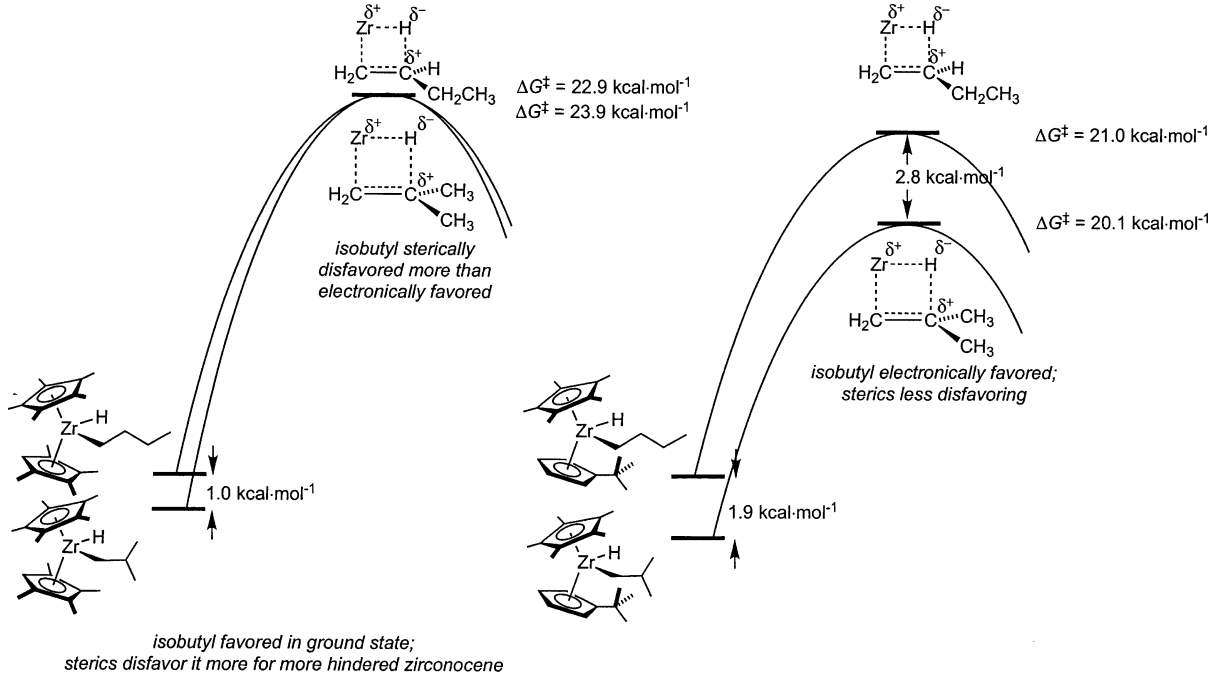

Figure 1. Free energy profiles for β-H elimination for Cp*(η^5-C_5Me_4H)Zr(CH_2CHMe_2)H (**19**) and Cp*(η^5-C_5Me_4H)Zr($CH_2CH_2CH_2CH_3$)H and for Cp*(η^5-C_5H_4-CMe_3)Zr(CH_2CHMe_2)H (**39**) and Cp*(η^5-C_5H_4-CMe_3)Zr($CH_2CH_2CH_2CH_3$)H, showing the relative ground-state and transition-state free energies for each pair.

β-H elimination for two different alkyls, both ground-state and transition-state effects must be considered. The relative ground-state energetics may be predicted on electronic grounds from the free energies of the alkanes, although increased cyclopentadienyl substitution slightly perturbs this value. For less substituted metallocenes, the electronic portion of the transition-state effect dominates and, as a result, the more β-substituted alkyl undergoes more facile β-H elimination.

The steric effects on the reverse process, olefin insertion, are generally much more sensitive, both to olefin and cyclopentadienyl substitution. Although chain transfer processes other than β-H elimination (e.g., β-methyl elimination, chain transfer to Al) may become favored, so that the issue is rather more complex, we conclude that increased molecular weight should be favored for less crowded metallocenes and less hindered olefins: olefin insertion responds more favorably to reduced unfavorable steric interactions than does chain transfer by β-H elimination.

Experimental Section

General Considerations. All air- and moisture-sensitive compounds were handled using standard vacuum line, Schlenk, or cannula techniques or in a drybox as described previously.[46] Argon, dinitrogen, dihydrogen, and dideuterium gases were purified by passage over columns of MnO on vermiculite and activated molecular sieves. Solvents for air- and moisture-sensitive reactions were stored under vacuum over titanocene[47] or sodium benzophenone ketyl. NMR solvents: benzene-d_6, toluene-d_8, tetrahydrofuran-d_8, diethyl ether-d_{10}, and pyridine-d_5 were purchased from Cambridge Isotope Laboratories. Benzene-d_6 and toluene-d_8 were dried over $LiAlH_4$ and sodium and then stored over titanocene. Tetrahydrofuran-d_8 and diethyl ether-d_{10} were dried over CaH_2 and stored over sodium/benzophenone ketyl. Pyridine-d_5 was dried over CaH_2. Preparations of **1**,[48] **2**,[24] **3**,[19] **20**,[19] **21**,[19] **22**,[19] **31**,[19] **32**,[19] and **33**[19] were accomplished as described previously.

Isobutene, 2-methyl-1-butene, 2,4-dimethyl-1-pentene, 2,3-dimethyl-1-pentene, and propylene were purchased from Aldrich. Isobutene and propene were dried over Al(*i*-Bu)$_3$ and distilled by vacuum transfer before use. The other olefins were distilled from CaH_2 and stored over $LiAlH_4$. Both *cis*- and *trans*-2-butene were purchased from Matheson and dried over activated 4 Å molecular sieves. Styrene and α-methylstyrene were purchased from Aldrich; *p*-fluoro-α-methylstyrene was purchased from Lancaster. All were distilled under reduced pressure from CaH_2 and stored frozen in the drybox. Preparations of *p*-methyl-α-methylstyrene, *p*-trifluoromethyl-α-methylstyrene, and *p*-methoxy-α-methylstyrene were accomplished by reaction of $Ph_3P{=}CH_2$ with the appropriate acetophenone as described previously,[49] and the resulting product was distilled at reduced pressure from CaH_2. Ferrocene used as an internal standard was purchased from Aldrich and sublimed before use.

NMR spectra were recorded on a Bruker AM500 (500.13 MHz for ^{1}H, 76.77 for ^{2}H, 125.77 MHz for ^{13}C) spectrometer. All chemical shifts are relative to TMS using ^{1}H (residual), ^{2}H, or ^{13}C chemical shifts of the solvent as a secondary standard. The temperature of the NMR probe was measured before and after each kinetic run with a standard CH_3OH reference tube.

Kinetics of the Reaction of 1 or 2 with Volatile Olefins. In the drybox, a J. Young NMR tube was charged with 0.50 mL of 0.0488 M (0.0244 mmol) stock toluene-d_8 solution of metallocene dihydride containing a known amount of ferrocene. The NMR tube was then attached to the vacuum line via a calibrated gas volume. The tube was evacuated at −78

(46) Burger, B. J.; Bercaw, J. E. In *Experimental Organometallic Chemistry*; ACS Symposium Series No. 357; Wayda, A. L., Darensbourg, M. Y., Eds.; American Chemical Society: Washington, DC, 1987; Chapter 4.

(47) Marvich, R. H.; Brintzinger, H. H. *J. Am. Chem. Soc.* **1971**, *93*, 2046.

(48) Schock, L. E.; Marks, T. J. *J. Am. Chem. Soc.* **1988**, *110*, 7701.

(49) Vogel, A. I. *Vogel's Textbook of Practical Organic Chemistry*, 5th ed.; John Wiley and Sons: New York, 1989; pp 495−498.

°C, 10 equiv of olefin was charged into the gas bulb by vacuum transfer, and the gas was condensed in the tube at −78 °C. The NMR probe was calibrated to the desired temperature, and the sample was shaken several times just before insertion into the probe. Approximately 10−15 spectra were recorded at regular intervals over the duration of 2−3 half-lives. Peak intensities of the ferrocene and metallocene dihydride were measured for each spectrum. The observed rate constants were obtained from slopes of plots of $\ln[Cp^*_2MH_2]$ versus time. Second-order rate constants were obtained by dividing the observed psuedo-first-order rate constants by the concentration of olefin. Activation parameters were obtained by measuring second-order rate constants over a temperature range. A plot of $\ln(k/T)$ versus $1/T$ resulted in a slope of $\Delta H^{\ddagger}/R$ and an intercept of $[(\Delta S^{\ddagger}/R) + 23.76]$. Reported errors in the rate constants represent one standard deviation from the least-squares fit of the experimental data. These errors were then used to determine the errors in the activation parameters.

Kinetics of the Reaction of 1 with Substituted α-Methylstyrenes. In the drybox, 0.25 mL of 0.096 M stock benzene-d_6 solution of **1** containing a known amount of ferrocene was charged into a J. Young NMR tube. Via microsyringe, 0.25 mL of a benzene-d_6 stock solution of α-methylstyrene was added to the tube, and the sample was then immediately frozen in liquid nitrogen. The tube was then quickly thawed and inserted into a NMR probe. Approximately 10−15 spectra were recorded at regular intervals over the duration of 2−3 half-lives. Workup of the data was carried out as described for the previous experiments.

Determination of *β*-H Elimination Rate Constants. In a typical experiment, a J. Young NMR tube was charged with 0.50 mL of a 0.0488 M stock benzene-d_6 or toluene-d_8 solution of zirconocene dihydride containing a known amount of ferrocene. On the vacuum line, the tube was frozen in liquid nitrogen and degassed with three freeze−pump−thaw cycles. Via a 6.9 mL calibrated gas volume, 100 Torr of the desired olefin was added at −196 °C. The tube was thawed and shaken. The ^{1}H NMR spectrum was then recorded to ensure that complete conversion to the alkyl hydride complex had occurred. The tube was reattached to the vacuum line, and via a 56.8 mL calibrated gas bulb, the desired amount of **37** was collected in the tube at −196 °C. The tube remained frozen in liquid nitrogen until insertion into the thermostated NMR probe. Approximately 10−15 spectra were recorded over regular intervals over the course of 2−3 half-lives. Workup of the data was carried out as described for the previous experiments.

Determination of Equilibrium Constants for Zirconocene Alkyl Hydride Complexes. In a typical experiment, a J. Young NMR tube was charged with 0.50 mL of 0.0488 M stock benzene-d_6 solution containing a known amount of ferrocene. On the vacuum line, the tube was degassed and the appropriate amount of isobutene and 1-butene was then added via calibrated gas volume. The tube was thawed and shaken thoroughly and allowed to stand at room temperature for several hours. The ^{1}H NMR spectrum was then recorded and the equilibrium constant computed from the integration of the various species in solution.

NMR Spectroscopic Data. $Cp^*_2Zr(CH_2CH(CH_3)CH_2CH_3)(H)$ (4). ^{1}H NMR (benzene-d_6): δ 1.92 (s, 30H, C_5Me_5); 6.31 (s, 1H, Zr*H*); −0.531 (dd, 1H, C*H*$_2$CH(CH$_3$)CH$_2$CH$_3$); 0.290 (dd, 1H, C*H*$_2$CH(CH$_3$)CH$_2$CH$_3$); *not located* (CH$_2$C*H*(CH$_3$)CH$_2$CH$_3$); 1.36 (m, 2H, CH$_2$CH(CH$_3$)C*H*$_2$CH$_3$); 0.877 (t, 7 Hz, 3H, CH$_2$CH(CH$_3$)CH$_2$C*H*$_3$); 1.76 (d, 5 Hz, 3H, CH$_2$CH(C*H*$_3$)CH$_2$CH$_3$). ^{13}C NMR (benzene-d_6): δ 12.83 (C_5Me_5); 118.26 (C_5Me$_5$); 70.28 (*C*H$_2$CH(CH$_3$)(CH$_2$CH$_3$); 31.17 (CH$_2$*C*H(CH$_3$)(CH$_2$CH$_3$); 22.87 (CH$_2$CH(CH$_3$)(*C*H$_2$CH$_3$); 13.52 (CH$_2$CH(CH$_3$)(CH$_2$*C*H$_3$); 29.09 (CH$_2$CH(*C*H$_3$)(CH$_2$CH$_3$).

$Cp^*_2Zr(CH_2CH(CH_3)CH_2CHMe_2)(H)$ (5). ^{1}H NMR (benzene-d_6): δ 1.94 (s, 30H, C_5Me_5); 6.39 (s, 1H, Zr*H*); −0.669 (dd, 1H, C*H*$_2$CH(CH$_3$)CH$_2$CHMe$_2$); 0.492 (dd, 1H, C*H*$_2$CH(CH$_3$)CH$_2$CHMe$_2$); 2.24 (m, 2H,CH$_2$C*H*(CH$_3$)CH$_2$CHMe$_2$); 1.12 (m, 2H, CH$_2$CH(CH$_3$)C*H*$_2$CHMe$_2$); 2.16 (m, 1H, CH$_2$CH(CH$_3$)CH$_2$CHMe$_2$); 1.02 (d, 6.5 Hz, 3H, CH$_2$CH(*CH*$_3$)CH$_2$CHMe$_2$); 0.98 (d, 6.5 Hz, 6H, CH$_2$CH(CH$_3$)CH$_2$CH(*CH*$_3$)$_2$). ^{13}C NMR (benzene-d_6): δ 12.30 (C_5Me_5); 12.50 (C_5Me_5); 117.34 (C_5Me$_5$); 117.71 C_5Me$_5$); 66.60 (*C*H$_2$CH(CH$_3$)CH$_2$CHMe$_2$); 39.09 (CH$_2$*C*H(CH$_3$)CH$_2$CHMe$_2$); 20.58 (CH$_2$CH(*C*H$_3$)CH$_2$CHMe$_2$); 22.64 (CH$_2$CH(CH$_3$)*C*H$_2$CHMe$_2$); 35.93 (CH$_2$CH(CH$_3$)CH$_2$*C*HMe$_2$); 13.53, 13.62 (CH$_2$CH(CH$_3$)CH$_2$CH(*C*H$_3$)$_2$).

$Cp^*_2Zr(CH_2CH(CH_3)CH(CH_3)CH_2CH_3)(H)$ (6). ^{1}H NMR (benzene-d_6): δ 1.93 (s, 30H, C_5Me_5); 6.35 (s, 1H, Zr*H*); −0.386 (dd, 1H, C*H*$_2$CH(CH$_3$)CH(CH$_3$)CH$_2$CH$_3$); 0.220 (dd, 1H, C*H*$_2$CH(CH$_3$)CH(CH$_3$)CH$_2$CH$_3$); 2.21 (m, 1H, CH$_2$C*H*(CH$_3$)CH(CH$_3$)CH$_2$CH$_3$); 1.31 (m, 1H, CH$_2$CH(CH$_3$)C*H*(CH$_3$)CH$_2$CH$_3$); 1.18 (m, 2H, CH$_2$CH(CH$_3$)CH(CH$_3$)C*H*$_2$CH$_3$); 1.01 (t, 7 Hz, 3H, CH$_2$CH(CH$_3$)CH(CH$_3$)CH$_2$C*H*$_3$).

$Cp^*_2Zr(CH_2CH(CH_3)(C_6H_5))(H)$ (7). ^{1}H NMR (benzene-d_6): δ 1.87 (s, 15H, C_5Me_5); 1.94 (s, 15H, C_5Me_5); 6.55 (s, 1H, Zr*H*); −0.944 (dd, 1H, C*H*$_2$CH(CH$_3$)(C$_6$H$_5$)); −0.969 (dd, 1H, C*H*$_2$CH(CH$_3$)(C$_6$H$_5$)); 1.56 (t, 6.5 Hz, 1H, CH$_2$C*H*(CH$_3$)(C$_6$H$_5$)); 1.65 (d, 7 Hz, 3H, CH$_2$CH(C*H*$_3$)(C$_6$H$_5$)); 7.42 (d, 7.1 Hz, 2H, CH$_2$CH(CH$_3$)(*ortho*-C$_6$*H*$_5$)); 7.11 (t, 7.5 Hz, 2H, CH$_2$CH(CH$_3$)(*meta*-C$_6$*H*$_5$)); 7.29 (t, 7.3 Hz, 1H, CH$_2$CH(CH$_3$)(*para*-C$_6$*H*$_5$)). ^{13}C NMR (benzene-d_6): δ 12.24 (C_5Me_5); 12.48 (C_5Me_5); 118.44 (C_5Me$_5$); 118.77 (C_5Me$_5$); 67.06 (*C*H$_2$CH(CH$_3$)(C$_6$H$_5$); 39.45 (CH$_2$*C*H(CH$_3$)(C$_6$H$_5$); 30.10 (CH$_2$CH(*C*H$_3$)(C$_6$H$_5$); 117.39, 117.65, 119.54, 123.75, 134.51, *1 not located* (*C*$_6$H$_5$).

$Cp^*_2Zr(CH_2CH_2CH_2CH_3)(H)$ (8). ^{1}H NMR (benzene-d_6): δ 1.89 (s, 30H, C_5Me_5); 6.27 (s, 1H, Zr-*H*); 0.159 (t, 9 Hz, 2H, C*H*$_2$ CH$_2$CH$_2$CH$_3$); 1.24 (m, 2H, CH$_2$ C*H*$_2$CH$_2$CH$_3$); 1.39 (m, 2H, CH$_2$ CH$_2$C*H*$_2$CH$_3$); 1.05 (t, 7.3 Hz, 3H, CH$_2$ CH$_2$CH$_2$C*H*$_3$). ^{13}C NMR (benzene-d_6): δ 12.09 (C_5Me_5); 113.00 (C_5Me$_5$); 52.48 (*C*H$_2$CH$_2$CH$_2$CH$_3$); 31.62 (CH$_2$*C*H$_2$CH$_2$CH$_3$); 25.57 (CH$_2$CH$_2$*C*H$_2$CH$_3$); 11.40 (CH$_2$CH$_2$CH$_2$*C*H$_3$).

$Cp^*_2Hf(CH_2CHMe_2)(H)$ (9). ^{1}H NMR (benzene-d_6): δ 1.95 (s, 30H, C_5Me_5); 9.76 (s, 1H, Hf-*H*); −0.25 (d, 6.5 Hz, 2H, C*H*$_2$ CHMe$_2$); 2.09 (m, 1H, CH$_2$ C*H*Me$_2$); 1.00 (d, 6 Hz, 6H, CH$_2$CH(C*H*$_3$)$_2$). ^{13}C NMR (benzene-d_6): δ 12.24 (C_5Me_5); 117.52 (C_5Me$_5$); 76.33 (*C*H$_2$CHMe$_2$); 31.94 (CH$_2$*C*HMe$_2$); 13.63 (CH$_2$CH(*C*H$_3$)$_2$).

$Cp^*_2Hf(cyclo\text{-}C_5H_9)(H)$ (10). ^{1}H NMR (benzene-d_6): δ 1.95 (s, 30H, C_5Me_5); 13.31 (s, 1H, Hf*H*); −0.17, 0.456, 1.08, 1.93, 2.27 (m, C$_5$*H*$_9$). ^{13}C NMR (benzene-d_6): δ 12.27 (C_5Me_5); 117.57 (C_5Me$_5$); 73.17 (C_1-cyclopentene); 29.86 (C_2-cyclopentene); 23.51 (C_3-cyclopentene).

$Cp^*_2Hf(CH_2CH_2C_6H_5)(H)$ (11). ^{1}H NMR (benzene-d_6): δ 1.88 (s, 30H, C_5Me_5); 12.96 (s, 1H, Hf*H*); −0.09 (t, 6.5 Hz, 2H, C*H*$_2$ CH$_2$Ph); 2.22 (t, 6.5 Hz, 2H, CH$_2$ C*H*$_2$Ph); 6.85 (m, 1H, *para*-CH$_2$CH$_2$C$_6$*H*$_5$); 6.98 (m, 2H, *meta*-CH$_2$CH$_2$C$_6$*H*$_5$); 7.34 (m, 2H, *ortho*-CH$_2$CH$_2$C$_6$*H*$_5$). ^{13}C NMR (benzene-d_6): δ 12.12 (C_5Me_5); 118.26 (C_5Me$_5$); 62.45 (*C*H$_2$CH$_2$Ph); 30.36 (CH$_2$CH$_2$Ph); 125.52 (*para*-*C*$_6$H$_5$); 137.50 (*ortho*-*C*$_6$H$_5$); 150.07 (*meta*-*C*$_6$H$_5$), *1 not located* (*ipso*-*C*$_6$H$_5$).

$Cp^*_2Hf(CH_2CH_2CH_2CH_3)(H)$ (12). ^{1}H NMR (benzene-d_6): δ 1.95 (s, 30H, C_5Me_5); 9.80 (s, 1H, Hf*H*); −0.005 (t, 9 Hz, 2H, C*H*$_2$ CH$_2$CH$_2$CH$_3$); *not located* (CH$_2$ C*H*$_2$CH$_2$CH$_2$CH$_3$); 0.981 (m, 2H, CH$_2$ CH$_2$C*H*$_2$CH$_3$); 1.06 (t, 7.4 Hz, 3H, CH$_2$ CH$_2$CH$_2$C*H*$_3$). ^{13}C NMR (benzene-d_6): δ 12.06 (C_5Me_5); 116.97 (C_5Me$_5$); 62.55 (*C*H$_2$CH$_2$CH$_2$CH$_3$); 31.50 (CH$_2$*C*H$_2$CH$_2$CH$_3$); 26.93 (CH$_2$CH$_2$*C*H$_2$CH$_3$); 14.76 (*C*H$_2$CH$_2$CH$_2$*C*H$_3$).

$Cp^*_2Hf(CH_2CH_2CH_2CH_2CH_3)(H)$ (13). ^{1}H NMR (benzene-d_6): δ 1.94 (s, 30H, C_5Me_5); 9.81 (s, 1H, Hf*H*); −0.005 (t, 9 Hz, 2H, C*H*$_2$ CH$_2$CH$_2$CH$_2$CH$_3$); *not located* (CH$_2$ C*H*$_2$CH$_2$CH$_2$CH$_3$); 0.991 (m, 4H, CH$_2$ CH$_2$C*H*$_2$C*H*$_2$CH$_3$); 1.12 (t, 7.4 Hz, 3H, CH$_2$ CH$_2$CH$_2$CH$_2$C*H*$_3$).

$Cp^*_2Zr(CH_2CH(CH_3)(C_6H_4\text{-}p\text{-}F))(H)$ (14). ^{1}H NMR (benzene-d_6): δ 1.84 (s, 15H, C_5Me_5); 1.86 (s, 15H, C_5Me_5); 6.31 (s, 1H, Zr*H*); −0.984 (dd, 1H, C*H*$_2$CH(CH$_3$)(C$_6$H$_4$-*p*-F)); −0.368 (dd, 1H, C*H*$_2$CH(Me)(C$_6$H$_4$-*p*-F)); 2.56 (m, 1H, CH$_2$CH(CH$_3$)(C$_6$H$_4$-*p*-F)); 1.78 (d, 3H, CH$_2$CH(C*H*$_3$)(C$_6$H$_4$-*p*-F)); 7.19 (m, 2H,

$CH_2CH(CH_3)$(*ortho*-C_6H_4-*p*-F)); 6.94 (m, 2H, $CH_2CH(CH_3)$-(*meta*-C_6H_4-*p*-F)).

Cp*$_2$Zr(CH$_2$CH(CH$_3$)(C$_6$H$_4$-*p*-CH$_3$))(H) (15). ^{1}H NMR (benzene-d_6): δ 1.89 (s, 15H, C_5Me_5); 1.94 (s, 15H, C_5Me_5); 6.54 (s, 1H, Zr*H*); 0.959 (dd, 1H, CH_2CH(CH_3)(C_6H_4-*p*-CH_3)); 0.912 (dd, 1H, CH_2CH(CH_3)(C_6H_4-*p*-CH_3)); 2.22 (m, 1H, $CH_2CH(CH_3)$-(C_6H_4-*p*-CH_3)); 1.19 (d, 7 Hz, 3H, $CH_2CH(CH_3)$(C_6H_4-*p*-CH_3)); 2.16 (s, 3H, $CH_2CH(CH_3)$(C_6H_4-*p*-CH_3)); 6.99 (d, 6 Hz, 2H, CH_2-CH(Me)(*meta*-C_6H_4-*p*-CH_3)); 7.34 (d, 6 Hz, 2H, $CH_2CH(CH_3)$-(*ortho*-C_6H_4-*p*-CH_3)).

Cp*$_2$Zr(CH$_2$CH(CH$_3$)(C$_6$H$_4$-*p*-OCH$_3$))(H) (16). ^{1}H NMR (benzene-d_6): δ 1.89 (s, 15H, C_5Me_5); 1.95 (s, 15H, C_5Me_5); 6.53 (s, 1H, Zr*H*); 0.904 (dd, 1H, CH_2CH(CH_3)(C_6H_4-*p*-OCH_3)); 0.912 (dd, 1H, CH_2CH(CH_3)(C_6H_4-*p*-OCH_3)); 1.62 (m, 1H, CH_2CH-(CH_3)(C_6H_4-*p*-OCH_3)); 1.78 (d, 6.5 Hz, 3H, $CH_2CH(CH_3)$(C_6H_4-*p*-OCH_3)); 3.34 (s, 3H, $CH_2CH(CH_3)$(C_6H_4-*p*-OCH_3)); 6.92 (d, 6 Hz, 2H, $CH_2CH(CH_3)$(*meta*-C_6H_4-*p*-OCH_3)); 7.34 (d, 6 Hz, 2H, $CH_2CH(CH_3)$(*ortho*-C_6H_4-*p*-OCH_3)).

Cp*$_2$Zr(CH$_2$CH(CH$_3$)(C$_6$H$_4$-*p*-CF$_3$))(H) (17). ^{1}H NMR (benzene-d_6): δ 1.84 (s, 15H, C_5Me_5); 1.92 (s, 15H, C_5Me_5); 6.54 (s, 1H, Zr*H*); −1.11 (dd, 1H, CH_2CH(CH_3)(C_6H_4-*p*-CF_3)); 0.053 (dd, 1H, CH_2CH(CH_3)(C_6H_4-*p*-CF_3)); 3.31 (m, 1H, $CH_2CH(CH_3)$-(C_6H_4-*p*-CF_3)); 1.05 (d, 6.8 Hz, 3H, $CH_2CH(CH_3)$(C_6H_4-*p*-CF_3)); 7.24 (d, 6 Hz, 2H, $CH_2CH(CH_3)$(*meta*-C_6H_4-*p*-CF_3)); 7.48 (d, 6 Hz, 2H, $CH_2CH(CH_3)$(*ortho*-C_6H_4-*p*-CF_3)).

Cp*(η^5-C$_5$Me$_4$H)Zr(CH$_2$CHMe$_2$)(H) (19). ^{1}H NMR (benzene-d_6): δ 1.91 (s, 15H, C_5Me_5); 1.60, 1.87, 2.10, 2.33 (s, 3H, C_5Me_4H); 4.52 (s, 1H, C_5Me_4H); 6.26 (s, 1H, Zr*H*); −0.445 (dd, 1H, CH_2CHMe$_2$); 0.443 (dd, 1H, CH_2CHMe$_2$); 2.15 (m, 1H, CH_2CHMe$_2$); 0.953 (d, 7 Hz, 3H, $CH_2CH(CH_3)_2$); 1.06 (d, 7 Hz, 3H, $CH_2CH(CH_3)_2$). ^{13}C NMR (benzene-d_6): δ 12.73 (C_5Me_5); 117.98 (C_5Me$_5$); 12.17, 12.32, 13.46, 14.56 (C_5Me_4H); 68.38 (CH_2CMe$_2$); 31.76 (CH_2CHMe$_2$); 24.47, 29.64 ($CH_2CH(CH_3)_2$); 111.51, 115.70, 119.70, 120.79, 121.63 (Cp).

Cp*(η^5-C$_5$Me$_4$CH$_2$CH$_3$)Zr(CH$_2$CHMe$_2$)(H) (23). ^{1}H NMR (benzene-d_6): δ 1.92 (s, 15H, C_5Me_5); 1.76, 1.79, 1.94, 1.98 (s, 3H, $C_5Me_4CH_2CH_3$); 1.85 (q, 6.5 Hz, 2H, $C_5Me_4CH_2CH_3$); 1.90 (t, 7 Hz, 2H, $C_5Me_4CH_2CH_3$); 6.34 (s, 1H, Zr*H*); −0.381 (dd, 1H, CH_2CHMe$_2$); 0.053 (dd, 1H, CH_2CHMe$_2$); 2.43 (m, 1H, CH_2CHMe$_2$); 0.82 (d, 7 Hz, 3H, $CH_2CH(CH_3)_2$); 1.10 (d, 7 Hz, 3H, $CH_2CH(CH_3)_2$).

Cp*(η^5-C$_5$H$_3$-(CMe$_3$)$_2$)Hf(CH$_2$CHMe$_2$)(H) (25). ^{1}H NMR (benzene-d_6): δ 1.98 (s, 15H, C_5Me_5); 1.22 (s, 9H, CMe_3); 1.48-(s, 9H, CMe_3); 12.98 (s, 1H, Hf*H*); −1.06 (m, 1H, CH_2CHMe$_2$); 0.75 (m, 1H, CH_2CHMe$_2$); 2.50 (m, 1H, CH_2CHMe_2); 1.04 (d, 7 Hz, 3H, $CH_2CH(CH_3)_2$); 1.17 (d, 7 Hz, 3H, $CH_2CH(CH_3)_2$); 4.92, 4.62, 6.50 (m, 1H, Cp). ^{13}C NMR (benzene-d_6): δ 12.71 (C_5Me_5); 116.96 (C_5Me$_5$); 32.34 (CMe_3); 32.99 (CMe_3); 145.06 (CMe_3); 145.96 (CMe_3); 76.44 (CH_2CHMe$_2$); 32.34 (CH_2CHMe$_2$); 24.33 ($CH_2CH(CH_3)_2$); 30.30 ($CH_2CH(CH_3)_2$); 99.86, 104.61, 105.64, *2 not located* (Cp).

Cp*$_2$Zr(CH$_2$CH$_2$C$_6$H$_5$)(H) (26). ^{1}H NMR (benzene-d_6): δ 1.88 (s, 30H, C_5Me_5); *not located* (Zr*H*); 0.54 (t, 6.9 Hz, 2H, CH_2CH$_2$Ph); 1.78 (t, 6.3 Hz, 2H, CH_2CH_2Ph); 7.08 (m, 1H, *para*-$CH_2CH_2C_6H_5$); 7.25 (m, 2H, *meta*-$CH_2CH_2C_6H_5$); 7.40 (m, 2H, *ortho*-$CH_2CH_2C_6H_5$). ^{13}C NMR (benzene-d_6): δ 12.18 (C_5Me_5); 117.51 (C_5Me$_5$); 51.79 ($CH_2CH_2C_6H_5$); 26.49 (CH_2CH_2-C_6H_5); 125.67, 126.15, 138.00, *1 not located* (C_6H_5).

Cp*{η^5-C$_5$H$_3$-1,3-(CMe$_3$)$_2$}Zr(CH$_2$CH$_2$C$_6$H$_5$)(H) (27). ^{1}H NMR (benzene-d_6): δ 1.89 (s, 15H, C_5Me_5); 1.16 (s, 9H, CMe_3); 0.956 (s, 9H, CMe_3); 6.49 (s, 1H, Zr*H*); −0.122 (td, 13.9 Hz, 3.8 Hz, 1H, CH_2 CH$_2$Ph); 0.693 (td, 13.9 Hz, 3.8 Hz, 1H, CH_2 CH$_2$Ph); 2.48 (td, 13.6 Hz, 4.8 Hz, 1H, CH$_2$ CH_2Ph); 2.86 (td, 13.6 Hz, 4.8 Hz, 1H, CH$_2$ CH_2Ph); 7.05 (m, 1H, *para*-CH_2-$CH_2C_6H_5$); 7.25 (m, 2H, *meta*-$CH_2CH_2C_6H_5$); 7.31 (m, 2H, *ortho*-$CH_2CH_2C_6H_5$); *not located* (*ipso*-C_6H_5).

{η^5-C$_5$H$_3$-1,3-(CMe$_3$)$_2$}$_2$Zr(CH$_2$CH$_2$C$_6$H$_5$)(H) (28). ^{1}H NMR (benzene-d_6): δ 1.28, (s, 9H, CMe_3); 1.45 (s, 9H, CMe_3); 5.33 (s, 1H, Zr*H*); 0.55 (t, 10 Hz, 2H, $CH_2CH_2C_6H_5$); 2.76 (t, 10 Hz, 2H, $CH_2CH_2C_6H_5$); 4.85, 5.22, 6.26 (s, 1H, Cp). ^{13}C NMR (benzene-d_6): δ 32.77 (CMe_3); 32.48 (CMe_3); 141.28 (CMe_3); 144.70 (CMe_3); 60.96 ($CH_2CH_2C_6H_5$); 34.29 ($CH_2CH_2C_6H_5$); 125.56, 126.95, 137.68, *1 not located* (C_6H_5); 97.41, 100.53, 106.63, 114.13, 122.65 (Cp).

Cp*(η^5-C$_5$H$_4$-CMe$_3$)Zr{CH(C$_6$H$_5$)(CH$_3$)}(H) (30). ^{1}H NMR (benzene-d_6): δ 1.75 (s, 15H, C_5Me_5); 1.83 (s, 15H, C_5Me_5); 1.11 (s, 9H, CMe_3); 1.36 (s, 9H, CMe_3);1.37 (s, 1H, Zr*H*); 5.40 (s, 1H, Zr*H*); −0.18 (d, 6.5 Hz, 3H, $CH(C_6H_5)(CH_3)$); 1.86 (d, 6.5 Hz, 3H, $CH(C_6H_5)(CH_3)$); *not located* ($CH(C_6H_5)(CH_3)$); 6.85, 6.89 (m, 1H, *para*-C_6H_5); 7.19, 7.25 (m, 2H, *meta*-C_6H_5); 7.39, 7.44 (m, 2H, *para*-C_6H_5); 3.18, 3.45, 3.66, 4.48, 4.62, 4.72, 4.77, 4.78 (Cp). ^{13}C NMR (benzene-d_6): δ 12.51, 12.85 (C_5Me_5); 114.30, 114.68, (C_5Me$_5$); 32.84, 32.88 (CMe_3); 136.62, 145.88 (CMe_3); 39.09, 47.91 ($CH(C_6H_5)(CH_3)$); −7.240, 17.68 ((CH-(C_6H_5)(CH_3)); 112.09, 123.75 (*para*-C_6H_5); 125.71, 126.73 (*ortho*-C_6H_5); 129.16, 132.36 (*meta*-C_6H_5); *2 not located* (*ipso*-C_6H_5); 99.98, 100.03, 100.10, 102.43, 104.08, 105.02, 110.04, 113.79, 120.77, 121.66 (Cp).

Cp*(THI)Zr(CH$_2$CH$_2$C$_6$H$_5$)(H) (34a). ^{1}H NMR (benzene-d_6): δ 1.86 (s, 15H, C_5Me_5); 5.89 (s, 1H, Zr*H*); 2.0−2.4 (m, THI); 0.706 (m, 2H, CH_2CH_2Ph); 0.870 (m, 2H, CH_2CH_2Ph); 6.94 (m, 1H, *para*-$CH_2CH_2C_6H_5$); 7.24(m, 2H, *meta*-$CH_2CH_2C_6H_5$); 7.37 (m, 2H, *ortho*-$CH_2CH_2C_6H_5$); 4.13, 4.57, 4.99 (Cp).

Cp*(THI)Zr((CH(C$_6$H$_5$)(CH$_3$))(H) (34b). ^{1}H NMR (benzene-d_6): δ 1.79 (s, 15H, C_5Me_5); *not located* (Zr*H*); 2.2−2.6 (m, THI); −0.90 (d, 8 Hz, 3H, $CH(C_6H_5)(CH_3)$); 1.20 (d, 8 Hz, 3H, CH-(C_6H_5)(CH_3)); 7.10 (m, 1H, *para*-$CH_2CH_2C_6H_5$); 7.22 (m, 2H, *meta*-$CH_2CH_2C_6H_5$); 7.29 (m, 2H, *ortho*-$CH_2CH_2C_6H_5$); 3.54, 4.58, 4.71, 4.90, *2 not located* (Cp).

(η^5-C$_5$Me$_4$H)$_2$Zr(CH$_2$CH$_2$C$_6$H$_5$)(H) (35a). ^{1}H NMR (benzene-d_6): δ 1.79, 1.82, 1.91, 1.99 (s, 6H, C_5Me_4); 6.47 (Zr*H*); 0.38 (t, 6.5 Hz, 2H, CH_2 CH$_2$Ph); *not located* (CH_2 CH_2Ph); 6.96 (m, 1H, *para*-$CH_2CH_2C_6H_5$); 7.35 (m, 2H, *meta*-$CH_2CH_2C_6H_5$); 7.40 (m, 2H, *ortho*-$CH_2CH_2C_6H_5$).

(η^5-C$_5$Me$_4$H)$_2$Zr((CH(C$_6$H$_5$)(CH$_3$))(H) (35b). ^{1}H NMR (benzene-d_6): δ 1.60, 1.66, 1.73, 1.79, 2.14, 2.15, 2.18, 2.32 (s, 6H, C_5Me_4H); 4.36, *1 not located* (s, 1H, Zr*H*); 0.485, *1 not located* (q, 6 Hz, 1H, C*H*(C_6H_5)(CH_3)); 1.26, *1 not located* ($CH(C_6H_5)$-(CH_3); 4.84, 4.89 (Cp).

Cp*{η^5-C$_5$H$_3$-1,3-(CHMe$_2$)$_2$}Zr(CH$_2$CH$_2$C$_6$H$_5$)(H) (36a). ^{1}H NMR (benzene-d_6): δ 1.82 (s, 15H, C_5Me_5); 0.51 (d, 7 Hz. 6H, $CHMe_2$); 0.84 (d, 7 Hz. 3H, $CHMe_2$); 0.88 (d, 7 Hz. 3H, $CHMe_2$); 1.07 (d, 7 Hz. 3H, $CHMe_2$); 2.45 (sept, 6.5 Hz, 1H, C*H*Me$_2$); 2.59 (sept, 6.5 Hz, 1H, C*H*Me$_2$); 6.42 (s, 1H, Zr*H*); −0.179 (m, 1H, CH_2 CH$_2$Ph); 0.82 (m, 1H, CH_2 CH$_2$Ph); 2.43 (m, 1H, CH$_2$ CH_2Ph); 2.84 (m, 1H, CH$_2$ CH_2Ph); 7.06 (m, 1H, *para*-CH_2-$CH_2C_6H_5$); 7.29 (m, 2H, *meta*-$CH_2CH_2C_6H_5$); 7.42 (m, 2H, *ortho*-$CH_2CH_2C_6H_5$); 4.89, 5.26, 5.45 (Cp).

Cp*{η^5-C$_5$H$_3$-1,3-(CHMe$_2$)$_2$}Zr(CH(C$_6$H$_5$)(CH$_3$))(H) (36b). ^{1}H NMR (benzene-d_6): δ 1.76 (s, 15H, C_5Me_5); 1.83 (s, 15H, C_5Me_5); 0.68 (d, 7 Hz. 3H, $CHMe_2$); 0.73 (d, 7 Hz. 3H, $CHMe_2$); 1.04 (d, 7 Hz. 3H, $CHMe_2$); 1.06 (d, 7 Hz. 3H, $CHMe_2$); 1.14 (d, 7 Hz. 3H, $CHMe_2$); 1.17 (d, 7 Hz. 3H, $CHMe_2$); 1.21 (d, 7 Hz. 3H, $CHMe_2$); 1.24 (d, 7 Hz. 3H, $CHMe_2$); *not located* (C*H*Me$_2$); 6.19, *1 not located* (s, 1H, Zr*H*); 4.25, 4.60, 4.63, 4.83, 4.89, 5.76 (Cp).

Cp*CpZr(CH$_2$CHMe$_2$)(H) (38). ^{1}H NMR (benzene-d_6): δ 1.89 (s, 15H, C_5Me_5); 6.22 (s, 1H, Zr*H*); −1.93 (dd, 1H, CH_2 CHMe$_2$); 0.25 (dd, 1H, CH_2 CHMe$_2$); 2.21 (m, 1H, CH$_2$ C*H*Me$_2$); 1.03 (d, 7 Hz, 3H, CH_2CHMe_2); 1.10 (d, 7 Hz, 3H, CH_2CHMe_2); 5.74 (s, 5H, C_5H_5). ^{13}C NMR (benzene-d_6): δ 12.18 (C_5Me_5); 117.62 (C_5Me$_5$); 71.65 (CH_2CHMe$_2$); 33.17 (CH_2CHMe$_2$); 29.91 (CH_2CHMe_2); 28.81 (CH_2CHMe_2); 111.07 (Cp).

Cp*(η^5-C$_5$H$_4$-CMe$_3$)Zr(CH$_2$CHMe$_2$)(H) (39). ^{1}H NMR (benzene-d_6): δ 1.86 (s, 15H, C_5Me_5); 1.34 (s, 9H, CMe_3); 6.22 (s, 1H, Zr*H*); −1.95 (dd, 1H, CH_2CHMe$_2$); 0.14 (dd, 1H, CH_2 CHMe$_2$); 2.41 (m, 1H, CH_2CHMe$_2$); 0.97 (d, 7 Hz, 3H, CH_2CH-(CH_3)$_2$); 0.99 (d, 7 Hz, 3H, $CH_2CH(CH_3)_2$); 4.87, 4.92, 5.41, 5.90 (Cp). ^{13}C NMR (benzene-d_6): δ 12.18 (C_5Me_5); 110.85 (C_5Me$_5$); 2.31 (CMe_3); 145.60 (CMe_3); 74.39 (CH_2CHMe$_2$); 33.53 (CH_2-CHMe$_2$); 28.20 ($CH_2CH(CH_3)_2$); 89.75, 98.92, 104.04, 107.98, 109.58 (Cp).

Cp*(THI)Zr(CH_2CHMe_2)(H) (40). ^{1}H NMR (benzene-d_6): δ 1.89 (s, 15H, C_5Me_5); 6.24 (s, 1H, Zr*H*); −1.67 (dd, 1H, CH_2-$CHMe_2$); 0.870 (dd, 1H, CH_2CHMe_2); 2.17 (m, 1H, CH_2CHMe_2); 0.975 (d, 7 Hz, 3H, $CH_2CH(CH_3)_2$); 1.04 (d, 7 Hz, 3H, CH_2CH-$(CH_3)_2$); 2.49, 2.55, 2.69, 2.78 (m, THI),4.70, 4.98, 5.61 (m, 1H, Cp). ^{13}C NMR (benzene-d_6): δ 12.70 (C_5Me_5); 117.39 (C_5Me_5); 24.32, 25.63, 26.18 28.47 (THI), 87.95 (CH_2CMe_2); 34.33 (CH_2CMe_2); 30.21 ($CH_2C(CH_3)_2$); 103.46, 105.21, 111.86, 126.45, 127.93 (Cp).

Cp*{η^5-C_5H_3-1,3-$(CHMe_2)_2$}Zr(CH_2CHMe_2)(H) (41). ^{1}H NMR (benzene-d_6): δ 1.92 (s, 15H, C_5Me_5); 6.34 (s, 1H, Zr*H*); 1.10 (d, 7 Hz. 3H, $CHMe_2$); 1.23 (d, 7 Hz. 3H, $CHMe_2$); 1.30 (d, 7 Hz. 3H, $CHMe_2$); 1.34 (d, 7 Hz. 3H, $CHMe_2$); 2.79 (sept, 6.5 Hz, 1H, $CHMe_2$); 3.25 (sept, 6.5 Hz, 1H, $CHMe_2$); −0.359 (dd, 1H, CH_2 $CHMe_2$); 0.220 (dd, 1H, CH_2 $CHMe_2$); 2.22 (m, 1H, CH_2 $CHMe_2$); 0.965 (d, 7 Hz, 6H, $CH_2CH(CH_3)_2$); 4.74, 4.85, 5.94 (m, 1H, C_5H_3-1,3-$CHMe_2$). ^{13}C NMR (benzene-d_6): δ 12.89 (C_5Me_5); 117.18 (C_5Me_5); 71.82 (CH_2CMe_2); 21.89, 22.64, 26.60, 27.34, 28.29, 29.07, 29.68, 30.48, 31.28 ($CHMe_2$, CH_2CMe_2); 88.31, 95.92, 100.52, 109.56, 123.00 (Cp).

Cp*{η^5-C_5H_3-1,3-$(CMe_3)_2$}Zr(CH_2CHMe_2)(H) (42). ^{1}H NMR (benzene-d_6): δ 1.88 (s, 15H, C_5Me_5); 6.48 (s, 1H, Zr*H*); 0.956 (s, 9H, CMe_3); 1.23 (s, 9H, CMe_3); −0.825 (dd, 1H, CH_2 $CHMe_2$); −0.836 (dd, 1H, CH_2 $CHMe_2$); 2.31 (m, 1H, CH_2 $CHMe_2$); 0.956 (d, 7 Hz, 6H, $CH_2CH(CH_3)_2$); 4.59, 4.75, 4.79 (m, 1H, C_5H_3-1,3-$(CMe_3)_2$). ^{13}C NMR (benzene-d_6): δ 12.89 (C_5Me_5); 117.86 (C_5Me_5); 32.06 (CMe_3); 33.03 (CMe_3); 2 *not located* (CMe_3); 70.44 ($CH_2CH_2Me_2$); 31.90 ($CH_2CH_2Me_2$); 31.32 (CH_2CH_2-$(CH_3)_2$); 29.98 ($CH_2CH_2(CH_3)_2$); 99.87,103.77, 105.82, 106.71, 116.87 (Cp).

(η^5-$C_5Me_4H)_2$Zr(CH_2CHMe_2)(H) (43). ^{1}H NMR (benzene-d_6): δ 2.01, 2.07 (s, 12H, C_5Me_4H); 5.10 (s, 2H, C_5Me_4H); 5.96 (s, 1H, Zr*H*); −0.06 (d, 6.8 Hz, 2H, CH_2CHMe_2); 2.28 (m, 1H, CH_2CHMe_2); 1.03 (d, 6 Hz, 6H, $CH_2CH(CH_3)_2$). ^{13}C NMR (benzene-d_6): δ 12.49, 13.14, 13.72, 14.22 (C_5Me_4H); 75.33 (CH_2CHMe_2); 31.17 (CH_2CHMe_2); 30.21 ($CH_2CH(CH_3)_2$); 108.37, 116.98, 117.45, 121.25, 121.76 (Cp).

Cp*(η^5-C_5Me_4H)Zr($CH_2CH_2C_6H_5$)(H) (44). ^{1}H NMR (benzene-d_6): δ 1.85 (s, 15H, C_5Me_5); 1.81, 1.84 (s, 6H, C_5Me_4H); 5.28 (bs, 1H, Zr*H*); −0.131 (m, 1H, CH_2CH_2Ph); 0.470 (m, 1H, CH_2CH_2Ph); *not located* (CH_2 CH_2Ph); 7.10 (m, 1H, *para*-$CH_2CH_2C_6H_5$); 7.24 (m, 2H, *meta*-$CH_2CH_2C_6H_5$); 7.42 (m, 2H, *ortho*-$CH_2CH_2C_6H_5$); 4.48 (Cp). ^{13}C NMR (benzene-d_6): δ 12.56 (C_5Me_5); 116.59 (C_5Me_5); 11.67, 12.19, 13.33, 14.71 (C_5Me_4H); 47.14 (CH_2CH_2Ph); 22.68 (CH_2CH_2Ph); 96.10, 105.77, 119.62, 2 *not located* (Cp); 122.42 (*para*-C_6H_5); 125.86 (*ortho*-C_6H_5); 129.40 (*meta*-C_6H_5); *1 not located* (*ipso*-C_6H_5).

Cp*(η^5-C_5Me_4H)Zr($CH_2CH_2(C_6H_4$-*p*-$OCH_3)$)(H) (45). ^{1}H NMR (benzene-d_6): δ 1.86 (s, 15H, C_5Me_5); 1.71, 1.77, 2.06, 2.10 (s, 6H, C_5Me_4H); 5.06 (s, 1H, Zr*H*); 0.51 (m, 2H, CH_2-$CH_2C_6H_5$-*p*-OCH_3); 1.52 (m, 2H, $CH_2CH_2C_6H_5$-*p*-OCH_3); 3.24 (s, 3H, $CH_2CH_2C_6H_5$-*p*-OCH_3); 6.88 (d, 8.6 Hz, 2H, CH_2CH_2-*meta*-C_6H_5-*p*-OCH_3); 7.36 (d, 8.6 Hz, 2H, CH_2CH_2-*ortho*-C_6H_5-*p*-OCH_3), 4.49 (Cp). ^{13}C NMR (benzene-d_6): δ 12.56 (C_5Me_5); 114.32 (C_5Me_5); 11.62, 12.23, 13.26, 14.78 (C_5Me_4H); 55.14 ($CH_2CH_2(C_6H_4$-*p*-$OCH_3)$); 20.35 ($CH_2CH_2(C_6H_4$-*p*-$OCH_3)$); 45.25 (C_6H_4−OCH_3); 105.56, 113.05, 116.18, 116.72, 117.09 (Cp); 122.01 (*ortho*-C_6H_4-*p*-OCH_3); 127.45 (*para*-C_6H_4-*p*-OCH_3); 130.32 (*meta*-C_6H_4-*p*-OCH_3); 159.16 (*ipso*-C_6H_4-*p*-OCH_3).

Cp*(η^5-C_5Me_4H)Zr($CH_2CH_2(C_6H_4$-*p*-$CH_3)$)(H) (46). ^{1}H NMR (benzene-d_6): δ 1.86 (s, 15H, C_5Me_5); 1.69, 1.79, 2.04, 2.11 (s, 6H, C_5Me_4H); 5.62 (bs, 1H, Zr*H*); 0.510 (m, 2H, CH_2-$CH_2C_6H_5$-*p*-CH_3); 1.57 (m, 2H, $CH_2CH_2C_6H_5$-*p*-CH_3); 6.94 (d, 8.6 Hz, 2H, CH_2CH_2-*meta*-C_6H_5-*p*-CH_3); 7.37 (d, 8.6 Hz, 2H, CH_2CH_2-*ortho*-C_6H_5-*p*-CH_3), 4.48 (Cp). ^{13}C NMR (benzene-d_6): δ 12.57 (C_5Me_5); 116.27 (C_5Me_5); 11.66, 12.19, 13.30, 14.76 (C_5Me_4H); 58.03 ($CH_2CH_2(C_6H_4$-*p*-$OCH_3)$); 29.21 (CH_2CH_2-$(C_6H_4$-*p*-$OCH_3)$); 38.06 (C_6H_4−CH_3); 113.04, 116.57, 116.84, 117.29, 117.82 (Cp); 122.28 (*ortho*-C_6H_4-*p*-CH_3); 137.97 (*para*-C_6H_4-*p*-CH_3); 143.97 (*meta*-C_6H_4-*p*-OCH_3); 159.03x (*ipso*-C_6H_4-*p*-CH_3).

(η^5-C_5Me_5)(η^5-C_5Me_4H)Zr($CH_2CH_2(C_6H_4$-*p*-$CF_3)$)(H) (47). ^{1}H NMR (benzene-d_6): δ 1.84 (s, 15H, C_5Me_5); 1.63, 1.77, 1.95, 2.16 (s, 6H, C_5Me_4H); 4.82 (s, 1H, Zr*H*); −0.237 (m, 1H, CH_2-$CH_2C_6H_5$-*p*-CF_3); 0.334 (m, 1H, C$H_2CH_2C_6H_5$-*p*-CF_3); 1.51 (m, 2H, $CH_2CH_2C_6H_5$-*p*-CF_3); 7.19 (d, 8.6 Hz, 2H, CH_2CH_2-*meta*-C_6H_5-*p*-CF_3); 7.48 (d, 8.6 Hz, 2H, CH_2CH_2-*ortho*-C_6H_5-*p*-CF_3), 4.48 (Cp). ^{13}C NMR (benzene-d_6): δ 12.50 (C_5Me_5); 116.16 (C_5-Me_5); 11.71, 12.06, 13.45, 14.54 (C_5Me_4H); 49.30 ($CH_2CH_2C_6H_4$-*p*-CF_3); 25.23 ($CH_2CH_2C_6H_4$-*p*-CF_3); 32.84 (q, 28 Hz, (CH_2-$CH_2C_6H_4$-*p*−CF_3); 106.29, 114.88, 115.87, 117.32, 119.43 (Cp); 125.67, 125.96, 141.44, *3 not located* ($CH_2CH_2C_6H_4$-*p*-CF_3). ^{19}F NMR (benzene-d_6): δ −62.19 ppm (CF_3).

Cp*(η^5-C_5H_4-CMe_3)Zr($CH_2CH_2CMe_3$)(H) (48). ^{1}H NMR (benzene-d_6): δ 1.89 (s, 15H, C_5Me_5); 1.47 (s, 9H, C_5H_4−CMe_3); *not located* (s, 1H, Zr*H*); −0.99 (m, 1H, C$H_2CH_2CMe_3$); 0.30 (m, 1H, C$H_2CH_2CMe_3$); 2.32 (m, 2H, $CH_2CH_2CMe_3$); 1.04 (s, 9H, $CH_2CH_2CMe_3$); 4.91 (m, 2H, Cp); 5.00 (m, 1H, Cp); 5.90 (m, 2H, Cp). ^{13}C NMR (benzene-d_6): δ 12.58 (C_5Me_5); 116.34 (C_5Me_5); 32.84 (CMe_3); 29.90 (CMe_3); 146.06 (CMe_3); 1 *not located* (CMe_3); 49.98 ($CH_2CH_2CMe_3$); 35.94 ($CH_2CH_2CMe_3$); 102.68, 104.01, 107.25, 109.89, 120.76 (Cp).

Cp*(η^5-C_5H_4-CMe_3)Zr($CH_2CH_2CH_2CHMe_2$)(H) (49). ^{1}H NMR (benzene-d_6): δ 1.83 (s, 15H, C_5Me_5); 1.41 (s, 9H, C_5H_4−CMe_3); 5.39 (s, 1H, Zr*H*); −0.450 (m, 1H, C$H_2CH_2CH_2CHMe_2$); −0.450 (m, 1H, C$H_2CH_2CH_2CHMe_2$); 0.651 (m, 2H, CH_2CH_2-CH_2CHMe_2); 0.589 (m, 2H, $CH_2CH_2CH_2CHMe_2$); 2.56 (m, 1H, $CH_2CH_2CH_2CHMe_2$); 0.999 (d, 6 Hz, 6H, $CH_2CH_2CH_2CH$-$(CH_3)_2$); 4.22, 4.91, 5.34, 5.98 (m, 1H, Cp). ^{13}C NMR (benzene-d_6): δ 12.46 (C_5Me_5); 112.77 (C_5Me_5); 32.09 (CMe_3); 139.36 (CMe_3); 56.14 ($CH_2(CH_2)_2CHMe_2$); 18.39, 22.29 ($CH_2(CH_2)_2$-$CHMe_2$) 32.78 ($CH_2(CH_2)_2CHMe_2$); 23.45 ($CH_2(CH_2)_2CH(CH_3)_2$; 103.56, 105.92, 109.53, 115.77, 118.64 (Cp).

Cp*(η^5-C_5H_4-CMe_3)Zr($CH_2CH_2CH_2CH_3$)(H) (50). ^{1}H NMR (benzene-d_6): δ 1.82 (s, 15H, C_5Me_5); 1.40 (s, 9H, CMe_3); 5.94 (s, 1H, Zr*H*); −0.504 (dd, 1H, C$H_2CH_2CH_2CH_3$); −0.02 (dd, 1H, C$H_2CH_2CH_2CH_3$); 1.26 (m, 2H, $CH_2CH_2CH_2CH_3$); 0.650 (m, 2H, $CH_2CH_2CH_2CH_3$); 1.06 (t, 7 Hz, 3H, $CH_2CH_2CH_2CH_3$); 4.23, 4.88, 4.91, 5.33 (Cp). ^{13}C NMR (benzene-d_6): δ 12.35 (C_5Me_5); 115.38 (C_5Me_5); 32.49 (CMe_3); 156.10 (CMe_3); 46.58 ($CH_2CH_2CH_2CH_3$); 29.56 ($CH_2CH_2CH_2CH_3$); 18.66 ($CH_2CH_2CH_2$-CH_3); 12.71 ($CH_2CH_2CH_2CH_3$); 101.09, 103.48, 104.00, 105.83, 109.43 (Cp).

Cp*(η^5-C_5H_4-CMe_3)Zr(*cyclo*-C_5H_9)(H) (51). ^{1}H NMR (benzene-d_6): δ 1.76 (s, 15H, C_5Me_5); 1.40 (s, 9H, C_5H_4−CMe_3); 5.71 (s, 1H, Zr*H*); −0.512, 0.105, 1.13, 1.93, 2.31 (m, C_5H_9); 4.73, 4.89, 4.96, 5.83 (m, 1H, Cp). ^{13}C NMR (benzene-d_6): δ 12.42 (C_5Me_5); 114.16 (C_5Me_5); 32.89 (CMe_3); 146.33 (CMe_3); 47.65 (*ipso*-C_5H_9); 23.51, 29.23, 34.10, 37.53 (C_5H_9); 99.90, 103.00, 104.41, 109.96, 125.51 (Cp).

Cp*CpZr{$C(CH_3)$=C(H)(CMe_3)}(H) (52). ^{1}H NMR (benzene-d_6): δ 1.81 (s, 15H, C_5Me_5); 3.51 (s, 1H, Zr*H*); 1.10 (s, 9H, C(CH_3)=C(H)(CMe_3)); 2.45 (s, 3H, C(CH_3)=C(H)(CMe_3); 3.45 (s, 1H, C(CH_3)=C(*H*)(CMe_3); 5.48 (Cp). ^{13}C NMR (benzene-d_6): δ 12.57 (C_5Me_5); 114.39 (C_5Me_5); 30.77 (C(CH_3)=C(CMe_3)-(H)); *not located* (C(CH_3)=C(CMe_3)(H)); 3.68 (C(CH_3)=C(CMe_3)-(H)); 186.82 (C(CH_3)=C(CMe_3)(H)); 95.71 (Cp).

Cp*(η^5-C_5H_4-CMe_3)Zr{$C(CH_3)$=C(H)(CMe_3)}(H) (53). ^{1}H NMR (benzene-d_6): δ 1.81 (s, 15H, C_5Me_5); 1.41 (s, 9H, C_5H_4−CMe_3); 3.54 (s, 1H, Zr*H*); 1.14 (s, 9H, C(CH_3)=C(H)(CMe_3)); 2.49 (s, 3H, C(CH_3)=C(H)(CMe_3); 3.48 (s, 1H, C(CH_3)=C(*H*)-(CMe_3); 4.52, 5.00, 5.08, 5.81 (Cp). ^{13}C NMR (benzene-d_6): δ 12.42 (C_5Me_5); 114.17 (C_5Me_5); 33.32 (CMe_3); 32.81 (CMe_3); 150.46 (CMe_3); 150.59 (CMe_3); 12.68 (C(CH_3)=C(CMe_3)(H)); 190.23 (C(CH_3)=C(CMe_3)(H)); 20.52 (C(CH_3)=C(CMe_3)(H)); 95.65, 95.94, 98.55, 99.07, 104.03 (Cp).

Cp*(THI)Zr{$C(CH_3)$=C(H)(CMe_3)}(H) (54). ^{1}H NMR (benzene-d_6): δ 1.84 (s, 15H, C_5Me_5); 0.80−1.10 (m, THI); 3.84 (s, 1H, Zr*H*); 1.24 (s, 9H, C(CH_3)=C(H)(CMe_3)); 2.49 (s, 3H, C(CH_3)=C(H)(CMe_3); 3.70 (s, 1H, C(CH_3)=C(*H*)(CMe_3); 4.98, 5.08, 5.55 (Cp). ^{13}C NMR (benzene-d_6): δ 12.60 (C_5Me_5); 114.31 (C_5Me_5); 31.90 (CMe_3); 159.11 (CMe_3); 3.77 (C(CH_3)=C(CMe_3)-

(H)); 187.12 (*C*(CH_3)=C(*C*Me_3)(H)); 20.17 (C(CH_3)=*C*(*C*Me_3)-(H)); 23.94, 24.58, 24.70, 26.86 (THI); 92.75, 100.32, 100.84, 101.83, 106.21 (Cp).

Cp*{η^5-C_5H_3-1,3-($CHMe_2$)$_2$}Zr(C(CH_3)=C(H)(CMe_3))-(H) (55). ^{1}H NMR (benzene-d_6): δ 1.85 (s, 15H, C_5Me_5); 3.68 (s, 1H, Zr*H*); 1.06 (d, 7 Hz. 3H, CHMe_2); 1.28 (d, 7 Hz. 3H, CHMe_2); 1.34 (d, 7 Hz. 3H, CHMe_2); 1.41 (d, 7 Hz. 3H, CHMe_2); 2.75 (sept, 6.5 Hz, 1H, C*H*Me_2); 3.20 (sept, 6.5 Hz, 1H, C*H*Me_2); 1.18 (s, 9H, C(CH_3)=C(H)(CMe_3)); 2.48 (s, 3H, C(CH_3)=C(H)-(CMe_3); 86.25 (*C*(CH_3)=C(*C*Me_3)(H)); 3.34 (s, 1H, C(CH_3)=C(*H*)(CMe_3); 4.65, 4.74, 4.98 (m, 1H, C_5H_3-1,3-(CMe_3)$_2$). ^{13}C NMR (benzene-d_6): δ 12.95 (C_5Me_5); 117.29 (*C*$_5$Me$_5$); 25.21, 25.48, 27.05, 27.26 (CHMe_2); 30.22, 21.14 (*C*HMe_2); 30.97 (CMe_3); 139.72 (*C*Me_3); 3.73 (C(*CH*$_3$)=C(CMe_3)(H)); *not located* (*C*(CH_3)=C(*C*Me_3)(H)); 21.90 (C(CH_3)=*C*(*C*Me_3)(H)) 88.37, 99.72, 99.42, 104.73, 114.49 (Cp).

Cp*{η^5-C_5H_3-1,3-(CMe_3)$_2$}Zr{C(CH_3)=C(H)(CMe_3)}(H) (56). ^{1}H NMR (benzene-d_6): δ 1.85 (s, 15H, C_5Me_5); 3.56 (s, 1H, Zr*H*); 1.17 (s, 9H, C_5H_5-1,3-(C*Me*$_3$)$_2$)); 1.55 (s, 9H, C_5H_5-1,3-(C*Me*$_3$)$_2$); 1.22 (s, 9H, C(CH_3)=C(H)(C*Me*$_3$)); 2.55 (s, 3H, C(C*H*$_3$)=C(H)(CMe_3); 3.34 (s, 1H, C(CH_3)=C(*H*)(CMe_3); 4.49, 4.68, 4.95 (m, 1H, C_5H_3-1,3-(CMe_3)$_2$). ^{13}C NMR (benzene-d_6): δ 13.06 (C_5Me_5); 119.88 (*C*$_5$Me$_5$); 32.88 (C*Me*$_3$); 32.20 (C*Me*$_3$); 114.16 (*C*Me_3); 117.44 (*C*Me_3); 31.88 (C*Me*$_3$); 136.18 (*C*Me_3); 3.83 (C(*CH*$_3$)=C(CMe_3)(H)); 167.31 (*C*(CH_3)=C(CMe_3)(H)); 28.04 (C(CH_3)=*C*(*C*Me_3)(H)); 100.99, 105.46, 109.02, *2 not located* (Cp).

Cp*(η^5-C_5Me_4H)Zr{C(CH_3)=C(H)(CMe_3)}(H) (57). ^{1}H NMR (benzene-d_6): δ 1.85 (s, 15H, C_5Me_5); 1.86, 1.88, 1.91, 2.01 (s, 3H, C_5Me_4 H); 4.47 (s, 1H, Zr*H*); 4.47 (s, 1H, C_5Me_4 *H*); 1.21 (s, 9H, C(CH_3)=C(H)(C*Me*$_3$)); 2.46 (s, 3H, C(C*H*$_3$)=C(H)(CMe_3); 3.53 (s, 1H, C(CH_3)=C(*H*)(CMe_3). ^{13}C NMR (benzene-d_6): δ 12.71 (C_5Me_5); 114.47 (*C*$_5$Me$_5$); 11.83, 12.41, 12.89, 13.32 (C_5Me_4H); 31.66 (C*Me*$_3$); 150.89 (*C*Me_3); 15.45 (C(*CH*$_3$)=C(CMe_3)(H)); 162.71 (*C*(CH_3)=C(*C*Me_3)(H)); 18.41 (C(CH_3)=*C*(*C*Me_3)(H)); 98.57, 102.25, 105.49, 122.54, *1 not located* (Cp).

(η^5-C_5Me_4H)$_2$Zr{C(CH_3)=C(H)(CMe_3)}(H) (58). ^{1}H NMR (benzene-d_6): δ 2.12, 2.21 (s, 6H, C_5Me_4H); 5.15 (s, 2H, C_5Me_4*H*); 3.73 (s, 1H, Zr*H*); 1.24 (s, 9H, C(CH_3)=C(H)(C*Me*$_3$)); 2.46 (s, 3H, C(C*H*$_3$)=C(H)(CMe_3); 3.35 (s, 1H, C(CH_3)=C(*H*)-(CMe_3). ^{13}C NMR (benzene-d_6): δ 12.11, 12.84, 13.96, 13.54 (C_5Me_4H); I88.33 (Zr−C(CH_3)=*C*(H)(CMe_3)); 187.30 (Zr-*C*(CH_3)=C(H)(CMe_3)); 31.56 (Zr−C(CH_3)=C(H)(C*Me*$_3$)); 143.72 (Zr−C(CH_3)=C(H)(*C*Me_3)); 18.64 (Zr−C(*C*H_3)=C(H)(CMe_3)); 98.95, 111.28, 114.82, 116.97, 120.26 (Cp).

Cp*CpZr($CH_2CH_2CH_2CH_3$)(H) (59). ^{1}H NMR (benzene-d_6): δ 1.73 (s, 15H, C_5Me_5); 6.21 (s, 1H, Zr*H*); −0.09 (dd, 1H, C*H*$_2$$CH_2CH_2CH_3$); 0.577 (dd, 1H, C*H*$_2$$CH_2CH_2CH_3$); 1.92 (m, 2H, CH_2 C*H*$_2$$CH_2CH_3$); 0.88 (m, 2H, CH_2 CH_2C*H*$_2$$CH_3$); 1.05 (t, 7.3 Hz, 3H, CH_2 CH_2CH_2C*H*$_3$), 5.91 (s, 5H Cp). ^{13}C NMR (benzene-d_6): δ 12.65 (C_5Me_5); 116.81 (*C*$_5$Me$_5$); 56.71 (*C*H_2CH_2-CH_2CH_3); 31.50 (CH_2*C*$H_2CH_2CH_3$); 24.95 (CH_2CH_2*C*H_2CH_3); 14.33 (*C*$H_2CH_2CH_2$*C*H_3); 107.16 (Cp).

Cp*{η^5-C_5H_3-1,3-($CHMe_2$)$_2$}Zr($CH_2CH_2CH_2CH_3$)(H) (60). ^{1}H NMR (benzene-d_6): δ 1.84 (s, 15H, C_5Me_5); 5.38 (s, 1H, Zr*H*); 1.19, 1.24, 1.42, 1.50 (d, 7 Hz, 3H, CHMe_2); 2.78, 3.20 (sept, 6.5 Hz, 1H, C*H*Me_2); −0.401 (m, 2H, C*H*$_2$ $CH_2CH_2CH_3$); *not located* (CH_2 C*H*$_2CH_2CH_3$); 1.06 (m, 2H, CH_2 CH_2C*H*$_2CH_3$); 0.870 (t, 7.3 Hz, 3H, CH_2 CH_2CH_2C*H*$_3$); 3.95, 4.88, 5.01 (m, 1H, Cp).

Cp*(THI)Zr($CH_2CH_2CH_2CH_3$)(H) (61). ^{1}H NMR (benzene-d_6): δ 1.86 (s, 15H, C_5Me_5); 5.95 (s, 1H, Zr*H*); −0.501 (m, 2H, C*H*$_2CH_2CH_2CH_3$); 1.40 (m, 2H, CH_2 C*H*$_2CH_2CH_3$); 0.82 (m, 2H, CH_2CH_2C*H*$_2CH_3$); 1.10 (t, 7.0 Hz, 3H, CH_2 CH_2CH_2C*H*$_3$), 4.75, 5.02, 5.20 (m, 1H, Cp). ^{13}C NMR (benzene-d_6): δ 12.15 (C_5Me_5); 117.92 (*C*$_5$Me$_5$); 23.84, 25.01, 25.25, 25.93 (THI); 53.40 (*C*H_2-$CH_2CH_2CH_3$); 47.52 (CH_2*C*$H_2CH_2CH_3$); 31.73 (CH_2CH_2*C*H_2-CH_3); 14.32 (*C*$H_2CH_2CH_2$*C*H_3); 107.65, 110.40, 111.60, 125.13, 125.76 (Cp).

Cp*(η^5-C_5Me_4H)Zr($CH_2CH_2CH_2CH_3$)(H) (62). ^{1}H NMR (benzene-d_6): δ 1.88 (s, 15H, C_5Me_5); 1.71, 1.81, 1.91, 2.08 (s, 3H, C_5Me_4 H); 4.47 (s, 1H, C_5Me_4*H*); 4.76 (s, 1H, Zr*H*); 0.057 (dd, 1H, C*H*$_2$ $CH_2CH_2CH_3$); 0.161 (dd, 1H, C*H*$_2$ $CH_2CH_2CH_3$); *not located* (CH_2C*H*$_2CH_2CH_3$); 1.43 (m, 2H, CH_2 CH_2C*H*$_2CH_3$); 1.08 (t, 6.5 Hz, 3H, $CH_2CH_2CH_2$C*H*$_3$). ^{13}C NMR (benzene-d_6): δ 12.60 (C_5Me_5); 115.71 (*C*$_5$Me$_5$); 11.67; 12.18; 12.30; 13.12 (C_5Me_4 H); 43.66 (*C*$H_2CH_2CH_2CH_3$); 27.86 (CH_2*C*$H_2CH_2CH_3$); 16.09 (CH_2CH_2*C*H_2CH_3); 15.06 (*C*$H_2CH_2CH_2$*C*H_3); 105.44; 115.56; 116.47; 116.89; 117.52 (Cp).

Cp*{η^5-C_5H_3-1,3-(CMe_3)$_2$}Zr($CH_2CH_2CH_2CH_3$)(H) (63). ^{1}H NMR (benzene-d_6): δ 1.72 (s, 15H, C_5Me_5); 1.10, 1.31 (s, 9H, C*Me*$_3$); 5.51 (s, 1H, Zr*H*); 0.14 (m, 2H, C*H*$_2$ $CH_2CH_2CH_3$); 0.652 (m, 2H, CH_2C*H*$_2CH_2CH_3$); 0.753 (m, 2H, CH_2CH_2C*H*$_2$-CH_3); 943 (t, 7 Hz, 3H, $CH_2CH_2CH_2$C*H*$_3$); 4.43, 4.60, 4.65 (m, 1H, Cp). ^{13}C NMR (benzene-d_6): δ 13.06 (C_5Me_5); 113.86 (*C*$_5$-Me$_5$); 32.86 (C*Me*$_3$); 35.00 (C*Me*$_3$); 142.62 (*C*Me_3); 140.92 (*C*Me_3); 42.13 (*C*$H_2CH_2CH_2CH_3$); 31.31 (CH_2*C*$H_2CH_2CH_3$); 27.38 (CH_2CH_2*C*H_2CH_3); 13.61 (*C*$H_2CH_2CH_2$*C*H_3); 100.99; 105.52; 109.05; 110.16; 111.99 (Cp).

Acknowledgment. This work has been supported by USDOE Office of Basic Energy Sciences (Grant No. DE-FG03-85ER13431), Exxon Chemicals America, and the National Science Foundation (Grant No. CHE-0131180).

OM0580351